INVESTIGATING THE REDUCTION OF FOGGING BEHAVIOR OF NATURAL FIBER-FILLED POLYMERS

A Thesis
Submitted to the Graduate Faculty
of the
North Dakota State University
of Agriculture and Applied Science

By

Nidhi Modha Thanki

In Partial Fulfillment of the Requirements
for the Degree of
MASTER OF SCIENCE

Major Department:
Materials and Nanotechnology

September 2021

Fargo, North Dakota

North Dakota State University
Graduate School

Title

INVESTIGATING THE REDUCTION OF FOGGING BEHAVIOR OF NATURAL FIBER-FILLED POLYMERS

By

Nidhi Modha Thanki

The Supervisory Committee certifies that this ***disquisition*** complies with North Dakota State University's regulations and meets the accepted standards for the degree of

MASTER OF SCIENCE

SUPERVISORY COMMITTEE:

Dr. Ali Amiri
Chair

Dr. Chad Ulven

Dr. Long Jiang

Dr. Mukund Sibi

Dr. Eric Hobbie

Approved:

September 29,2021
Date

Dr. Eric Hobbie
Department Chair

ABSTRACT

Synthetic fibers such as glass and carbon are used as reinforcement in polymer composites due to their high strength and modulus. However, synthetic fibers are non-biodegradable and contribute to high costs. In literature, various natural fibers, including banana and sisal fiber, as reinforcement in a polymer matrix, are investigated for mechanical and thermal properties to overcome this challenge. Nevertheless, natural fibers bring their issues such as degradation and emissions of Volatiles Organic Compounds (VOCs), resulting in the fogging phenomena when exposed to heating-cooling cycles. In this study, effectiveness of addition of porous fillers in reducing VOCs emissions in biocomposites reinforced with natural fibers is investigated. Mechanical testing exhibited that adding the porous filler into the biocomposites did not hinder mechanical properties. It is hypothesized that adding the porous filler in the biocomposites could reduce the VOCs emission due to the pore structures absorbing the VOCs.

ACKNOWLEDGMENTS

I would like to thank my advisor, Dr. Ali Amiri, for all the great advice and patience throughout my research. I would also like to thank my committee member, Dr. Chad Ulven, Dr. Long Jiang, Dr. Mukund Sibi, and Dr. Eric Hobbie, for serving my master thesis committee.

I would like to thank the North Dakota State University research team that helped with equipment training and processing trials. I also would like to thank Abigail Henderson, an undergraduate research assistant, for helping in materials processing and making the specimen for the tests.

I would like to thank the CB^2 and mentors for providing the financial support to carry out this study successfully.

TABLE OF CONTENTS

LIST OF TABLES

LIST OF FIGURES

LIST OF APPENDIX TABLES

LIST OF APPENDIX FIGURES

1. BACKGROUND AND INTRODUCTION

Composites, made from combining two or more materials, often polymer matrix filled with fibers, are widely used in the automotive industry, construction, or other industries [1]. Polypropylene (PP) is the most widely used plastic in the automobile industry as the polymer matrix. PP has an excellent cost-performance ratio and material properties [2]. However, recycling these plastics is complex as their compositions are made of petroleum-based polymer [3]. Hence, environment-conscious bodies across the world are advocating for the creation and implementation of policies and regulations compelling the automotive industry to use more sustainable materials that are easy to recycle [4]. As a result, the global automobile industry is under increased pressure to use sustainable materials in manufacturing vehicles. In response to the world's demand to embrace sustainable materials for production, the automobile industry is slowly embracing the use of natural fibers such as biocomposites.

Biocomposites are defined as polymer matrices reinforced with natural fibers such as flax, jute, ramie, sisal, coir, oil palm, and kenaf fibers [5–8]. Animals, plants, and mineral resources such as igneous rocks rich in magnesium silicates are the primary source of the natural fibers [9,10]. The use of natural fibers as a reinforcement in plastics delivers many advantages, such as cost reduction, improving mechanical properties, environment friendliness, reduced CO_2 emission, and enhanced biodegradation [11–13]. The outlined benefits of natural fiber have drawn researchers' attention to the study of the impact of incorporating natural fibers into plastics, particularly in developing more environmentally friendly composites [13–16].

1.1. Natural Fibers

Plant fibers are classified into bast, leaf, seed, stalk, grass, and other crop residue and wood fibers [17]. Fibers are attained from the outer bark stem of various plants, known as bast fibers.

Usually, these fibers are extracted through the retting process [17]. Some bast fibers, especially those comprising flax, hemp, jute, and ramie, have a high level of durability and tensile strength (see Table 1 below) [18]. On the other hand, Leaf fibers are extracted through hand scraping after the beating/retting process or mechanical extraction from the leaf tissues [17]. Sisal, date palm, abaca, and pineapple are some of the examples of leaf fibers. Wood fibers are another example of natural fibers. Wood fibers are abundant in supply since they are sourced from various trees. They are classified into two main categories: softwood and hardwood fibers [17]. The difference between hardwood and softwood is that hardwood has complex structures compared to softwood [19]. These types of fiber are processed at industrial sources such as sawmills in the form of wood chips.

Table 1. Mechanical Properties of Natural Fibers found in literature[19–21]

Category	**Fiber Type**	**Density (g/cm3)**	**Diameter (µm)**	**Length (mm)**	**Strength (MPa)**	**Modulus (GPa)**	**Elongation at Break (%)**
Bast	Flax	1.5–1.54	–	5–900	450–1500	27.6–38	1.5–3.2
	Ramie	1.45	34	900–1200	400–938	24.5–128	1.2–3.8
	Hemp	1.48	53.7	5–55	690–873	9.93	1.6–4.7
	Jute	1.3–1.45	25–200	1.5–120	393–773	2.5–26.5	1–2
Leaf	Sisal	1.45	50–200	900	80–640	1.46–15.8	3–15
	Date palm	0.92	100–1000	–	170–275	5–12	5–10
	Abaca	1.5	28	–	756	31.1	2.9
Wood	Softwood	0.3–0.88	16	–	51–120.7	5.2–15.6	–
	Hardwood	0.3–0.59	30	–	45.5–111.7	3.6–14.3	–

Natural fibers are made up of cellulose microfibrils in helical form with the matrix of hemicelluloses and lignin [21]. The constituents of natural fiber vary depending on a wide range of factors, among them the age of plants, growing conditions, plant types, and plant species [19]. Generally, the mechanical performances of the composites reinforced with natural fibers depend on the physical and chemical properties of the natural fibers [19].

Flax fiber is one of the most common bast fibers used in the biocomposite. It is a cellulose polymer with a crystalline structure, thus making it stronger and stiffer to handle [22]. The primary chemical components of the flax fibers are lignin, pectin, cellulose, and hemicellulose [22]. The physical properties of the flax fiber are dependent on cellulose, hemicellulose, and lignin [22]. According to a study by Garkhail *et al.* [23], the average tensile strength and modulus of PP range from 35MPa to 40MPa and 7GPa to 8GPa, respectively. In this study, the influence of the maleic-anhydride grafted polypropylene (MAPP) on interfacial adhesion and the mechanical properties of the composites are also investigated. The study infers that adding the 5% wt. of the MAPP does not affect the tensile properties of the PP/Flax composite.

Similarly, Van Den Oever *et al*. [24] investigated the influence of the physical structure of flax fibers on the mechanical properties of the flax fiber that is reinforced with polypropylene. The study established that polypropylene reinforced with flax fiber produced tensile strength ranging from 35MPa to 42MPa, and a tensile modulus averaging between 3.5-4.1GPa [24]. In addition, the average flexural strength and flexural modulus, as outlined in the research by Van Den Oever *et al*. [24], were between 60MPa to 70MPa and 4.5GPa to 6.5GPa, respectively. The study also examined the influence of the MAPP on the mechanical properties of flax fiber. The research by Van Den Oever *et al*. [24] concluded that hackled flax/PP with MAPP increased the mechanical properties of the components as compared to scutched flax/PP. Thus, it is justifiably inferable from the study's findings that the difference in the type of the natural fiber-reinforced composite and the method adopted for its processing has a considerable influence on the composite's mechanical properties.

On the contrary, a research study by Singleton *et al*. [25] investigated the impact of fiber volume fraction on the flax fiber/recycled high-density polyethylene (HDPE) laminate

manufactured by a hand lay-up and compression molding technique. The tensile test revealed that increasing the fiber volume fraction by 0%, 10%, 18%, 20%, and 30% led to the subsequent increase in the tensile strength and modulus, with the fiber volume fraction increased by 30% producing the highest tensile property Singleton *et al*. [25]. At the same time, the Charpy impact test exhibited the higher impact energy at 10% fiber volume fraction (Singleton *et al*.) [25]. Therefore, it was concluded from this study that the optimum fiber volume fraction should be between 15 and 20% to guarantee the attainment of maximum mechanical properties. In contrast, Bodros *et al*. [26] examined the mechanical properties of the biopolymeric matrix such as polycaprolactone and starch thermoplastic (Mater-Bi®ZF03U/A), poly(butylene succinate) (PBS), poly(butylene adipate-co-terephthalate) (PBAT), polylactic acid (PLA), l-polylactide acid (PLLA), and poly(3-hydroxyl butyrate) (PHB), reinforced with the flax fiber. The research has proven that the film stacking process offered the advantage of reducing fiber degradation during the process. Furthermore, it is noteworthy that the highest tensile properties reported for the PLLA/flax fibers showed promising results adoptable in structural application.

Like flax fibers, wood fibers have been used to reinforce thermoplastics for decades. Pine and maple are the most commonly used wood fibers for reinforcing thermoplastics. The chemical and physical properties of the wood fibers depend on the types of wood species used for extracting the fibers. As noted earlier in this research, the primary chemical constituents of the wood fiber are cellulose, hemicellulose, and lignin. However, the chemical composition of wood fibers differs based on the wood species used [27]. For instance, a study by Li *et al*. [28] explores the mechanical and structural properties of the HDPE/ionomer reinforced with the maple fibers. Li *et al*. [28] found that the highest flexural strength was reported between 26MPa and 30MPa, while the highest flexural modulus was reported between 55GPa and 60GPa. Additionally, Li *et al*. [28] explain that

the structural properties of biocomposites are classified using creep, differential scanning calorimetry (DSC), and DMA experiments. Those experiments suggested that ionomer modified the wood-polymer interface by developing immiscible morphology Li *et al*. [28].

Yen *et al*. [29] investigated the influence of the extruder process variables on the PP reinforced with maple fiber and their mechanical properties. In this study, it was found that the highest tensile properties reported for the composite had 85rpm counter-rotation, 42.89MPa tensile strength, and 5.07GPa for tensile modulus (Yen *et al*. [29]). Nonetheless, it was observed from the research that changing the extrusion process did not improve the mechanical properties of the composites (Yen *et al*. [29]). Kim *et al*. [30] examined the effect of the different wood species on the mechanical and thermal properties of the wood-plastic composites (WPCs). The research established that mechanical testing suggested that the wood species do not impact the tensile properties of the WPCs (Kim *et al*. [30]). Moreover, Kim *et al*. [30] observed that dynamic mechanical properties were dependent on the crystallization behavior of the wood flour, which is directly related to the extent to which the wood surfaces are rough.

Teymoorzadeh *et al*. [31] examined the influence of the maple wood flour content on the mechanical and thermal properties of the PLA-based composites. It was established from the study by Teymoorzadeh *et al*. [31] that increasing the wood fiber content enhanced its mechanical properties. Additionally, the study found that adding wood fiber content reduces the glass transition, crystallinity, and melting temperature of the composites, hence enhancing their mechanical properties. Another study by Murayama *et al*. [32] investigated the mechanical properties of polypropylene reinforced with pine wood flour (WF) produced by wet-ball milling under the various milling times and drying methods. This research found that the drying method does not affect the mechanical properties of wood flour (Murayama *et al*. [32]). However, the

study showed that the strength of the wood fiber increased significantly as the milling time increased (Murayama *et al*. [32]). This finding is justified by the fact that the increase in milling time produces decreased WF particles size, which has stronger cohesive power than the larger particles.

Stark *et al*. [33] investigated how the particle size of pine wood flour affects the mechanical properties of the pinewood flour/PP composites. Stark *et al*. [33] found that adding 40% wood flour to PP/MAPP increased the tensile strength by 27%, tensile modulus by 6%, and flexural strength by 20%. However, the study found that flexural modulus did not change with increasing the wood flour content (Stark *et al*. [33]). Furthermore, the study showed that the particle size of the wood flour did not influence its strength and stiffness (Stark *et al*. [33]).

Qiang *et al*. [34] studied the effects of linear low-density polyethylene (LLDPE) on the PLA/pine plastic composites. The static and dynamic mechanical and thermal properties of the PLA/pine composites were also examined in the study (Qiang *et al*. [34]). The research found that PLA composites modified with LLDPE produced a high impact strength, elongation at the break, and storage modulus but diminished tensile strength (Qiang *et al*. [34]).

Table 2 below summarizes the mechanical properties of the natural fiber composites and their potential application reported in the literature review by the other researchers. It can be observed from the table below that fiber type, origin, and matrix influenced the mechanical properties of the natural fiber composites.

Table 2. Average tensile and flexural properties of the natural fiber composites reported by the researchers

Fiber Type/ (Origin)	Matrix	Fiber content	Avg. Tensile Properties	Avg. Flexural Properties	Processing	Application	Ref.
Non-woven flax fiber (Netherland)	PP	10–50%	35–40MPa 7–8GPa	–	Film-stacking method and a suspension impregnation	Low-cost engineering	[23]
Scutched and hackled flax fiber (–)	PP Fiber	20 and 40%	35–42MPa 3.5-4.1GPa	60–70MPa 4.5–6.5GPa	Wet-laid process	Automotive sector	[24]
Flax fiber mat (–)	HDPE	10, 18, 20, and 30%	40–45 MPa 8–10GPa	–	Hand lay-up and compression molding	–	[25]
Dew-retted flax fiber (France)	Bio-polymer	20, 25, and 30%	95–105 MPa 8–10GPa	–	Film stacking method	Structural	[26]
Maple flour (American wood fiber)	HDPE/ionomer blends	60%		26–30MPa 55–60GPa	Mixed in roller mixer then compression-molded	–	[28]
Maple flour (American wood fiber)	PP	50%	42.89 MPa 5.07GPa	–	twin-screw extruder	Building	[29]
Pine and maple flour (American wood fiber)	PP	50%	24–28MPa 2.8–3.7GPa	–	co-rotating twin-screw extruder and injection mold	–	[30]
Maple flour (Université Laval)	PLA	15, 25 and 40%	–	5–6GPa	Extrusion and injection molding	–	[31]

Table 2. Average tensile and flexural properties of the natural fiber composites reported by the researchers (continued)

Fiber Type/ (Origin)	Matrix	Fiber content	Avg. Tensile Properties	Avg. Flexural Properties	Processing	Application	Ref.
Red Pine flour (Japan)	PP	25%	50–55Mpa 3.25–3.5GPa	–	Micro-compounder and injection molding	–	[32]
Pine flour (American wood fiber)	PP	20 and 40%	25.5MPa 3.61GPa	42.9MPa 3.15GPa	twin-screw extruder and injection mold	–	[33]
Pine flour (China)	PLA and LLDPE	10, 20, and 30%	60-65Mpa	–	twin-screw extruder and injection mold	automotive industry and in civil engineering	[34]

Note: The highest mechanical properties on average are reported in this table.

Based on studies conducted on the flax, maple, and pine fibers, it can be concluded that natural fibers can be used in composites in the place of synthetic fibers. However, the use of natural fillers as reinforcement in plastics comes with its challenges. For example, one of the main concerns with using natural fiber-filled plastic in the interior compartments and parts of a vehicle is fogging phenomenon and VOCs emissions. Another challenge of using natural fiber composites is that fiber and polymer both display time-dependent properties. Thus, the long-term creep behavior of these composites is critical due to the increased use in structural application.

1.1.1. Fogging Behavior

The fogging phenomenon is defined as forming Volatile Organic Compounds (VOCs) on windows from the material inside the cabin due to high/low-temperature cycles. Over time, these VOCs can condensate on the windshield, decrease the driver's visibility, and contribute to indoor pollution [35,36]. During high temperatures, the polymer goes through oxidation and random chain scission [37]. Chain scission results in radical production or the loss of low molecular weight or highly volatile compounds [38]. Polypropylene is made of the propylene monomer consists of the 3-carbon alkyl organic compound via the addition polymerization [39]. Figure 1 represents the schematic diagram of the chemical structure of the polypropylene after the addition polymerization process.

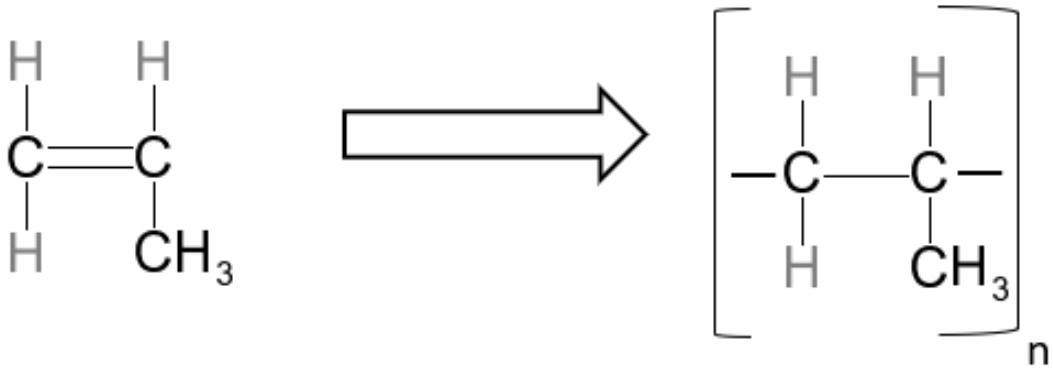

Figure 1. Chemical structure of the polypropylene

Note: Redrawn in the Chem4word.

As PP goes under thermal degradation in the inert environment, volatile compounds such as methylated alkane and alkenes are formed and escape the polymeric matrix as emission due to the low molecular weight [2,40]. The primary constituent of the petroleum-based polymer is an alkane, saturated hydrocarbons, and waxy in structure [41]. Alkenes, an unsaturated hydrocarbon, is another major constituent present in the petroleum-based polymer [42]. Figure 3 represents the schematic chemical structure of the alkane and alkenes used in the petroleum-based polymers.

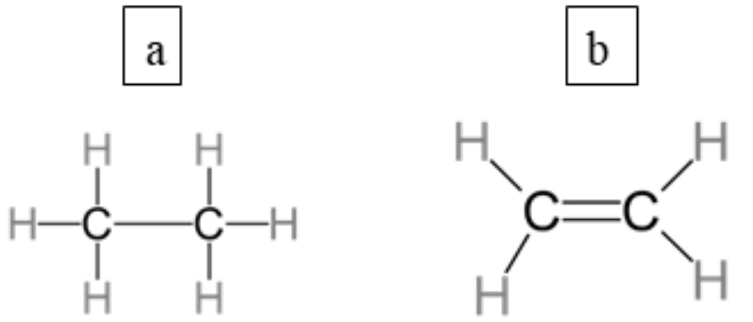

Figure 2. Chemical structure of (a) alkane and (b) alkenes

Note: Redrawn in the Chem4word.

As mentioned before, the main three components of natural fibers are cellulose, hemicellulose, and lignin [21]. Cellulose, Figure 3.a, is a type of natural crystalline polymer made up of the repeating monomer D-anhydro glucose connected with the 1,4-β-D-glycosidic unit. This repeating monomer unit has three hydroxyl groups [16,19]. Cellulose I_α and cellulose I_β are two types of the existing cellulose in nature. In all species of the plate, cellulose I_β is present [16,19]. Cellulose is resistant to oxidizing agents and strong alkali; however, it can easily be hydrolyzed by acid.

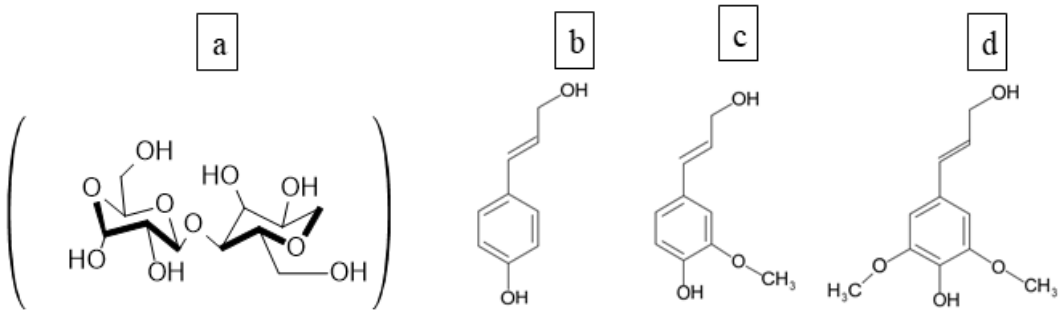

Figure 3. (a) Cellulose and phenolic monomers (b) p-coumaryl alcohol, (c) coniferyl alcohol, and (d) sinapyl alcohol

Note: Redrawn in the Chem4word and Chemsketch.

Another component of the natural fiber is hemicellulose, a matrix of polysaccharides [16]. Hemicellulose is different from cellulose in many ways. For example, hemicellulose comprises several distinct sugar units, an amorphous branched polymer, and has a low degree of polymerization [16,19]. In addition, hemicellulose has low thermal stability compared to cellulose and lignin [15]. The last major component in the natural fiber is lignin. Lignin is an amorphous phenolic polymer that contains the aromatic and aliphatic constituents produced by the phenyl propane units (Figure 3.b) [16,19]. Lignin plays a role in binding the cellulose and hemicellulose together [16]. It is not hydrolyzed by acids; however, soluble in hot alkali and readily oxidized [16]. Other minor constituents of the natural fibers are protein, fat, waxes [21]. The degradation process starts with the evaporation of the water combined with the emission of the volatile components; as the temperature is elevated, the char formation takes place [15]. Phase I of this project found that crude protein and hydroxyl group present (Figure 4) in the natural fibers contribute to the fogging behavior in the biocomposites.

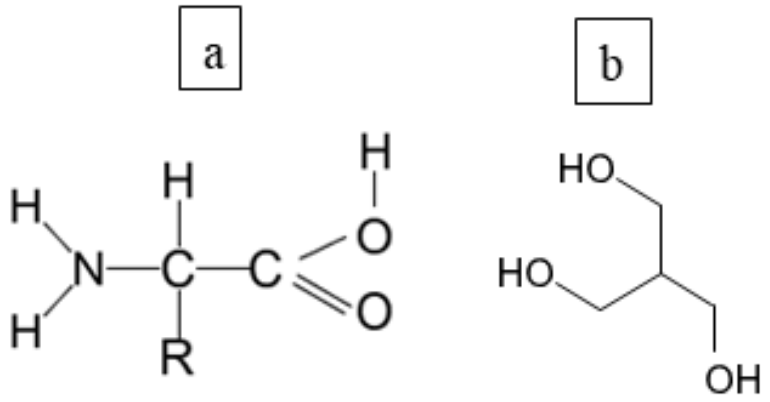

Figure 4. Molecular structure of the (a) protein and (b) hydroxyl group

Note: Redrawn in the Chem4word and Chemsketch.

To assess what types of compounds are being emitted, many analytical techniques such as gas chromatography-mass spectrometry (GC-MS), microwave-assisted extraction (MAE)-GC-

MS, simultaneous pyrolysis methylation (SPM)-GC-MS, and thermogravimetric analysis (TGA)-GC-MS have been used by the researcher to analyze the VOCs emissions from the polymer [43].

1.1.2. Creep

In the applications of material where it has to sustain external load for a long time, it is essential to measure the creep behavior [44]. This creep phenomenon describes as the inclination of the polymer deformation due to load and temperature. When constant stress is applied to the polymer, chains start to uncoil and slip past each other resulting in the deformation of the polymer matrix [44]. Additionally, creep behavior is time-dependent and requires a long time to perform tests [45,46]. Therefore, many researchers have predicated creep behavior by modeling the long-term creep behavior using the time-temperature superposition method (TTS) [13,45]. Williams–Landel–Ferry (WLF) is the most common empirical equation used in TTS for the composites materials, which relates a shift in temperature with a shift in time [46].

$$log a_T = \frac{-C_1(T - T_0)}{C_2 + (T - T_0)} \quad (1)$$

C_1 and C_2 are empirical constants that depend on the material properties, and T_0 (K) is the reference temperature.

Another equation used in the TTS is the Arrhenius equation which relates the rate of reaction and temperature [46] and generally Arrhenius equation is applied to the semicrystalline polymer [45]. Arrhenius equation is described as below:

$$log a_T = \frac{E}{R}\left(\frac{1}{T} - \frac{1}{T_0}\right) \quad (2)$$

Where a_T is the horizontal (or time) shift factor, R is the universal gas constant (J/mol. K), T_0 is the reference temperature (K), E is the activation energy (kJ/mol), and T (K) is the temperature at which a_T is desired.

To generate the master creep compliance curve of the biocomposites, empirical models such as Fit Findley Power Law is being used by many researchers [45]. Findley Power Law [47], the time-dependent creep compliance of materials can be represented by as :

$$J(t) = At^n \quad (3)$$

Where A is the time-dependent coefficient and it is y intercepts at 1 hours, t is the time (s), and n is exponents and the stress-independent coefficient [48]. This equation can be expressed as:

$$J = J_0 + J(t) = J_0 + At^n \quad (4)$$

Where J_0 is the time-independent or elastic creep compliance (1/MPa), and it is referred to as the Findley Power Law equation.

2. LITERATURE REVIEW

Due to the recent trend in the automotive and building sector in which manufacturers are shifting towards the use of sustainable materials on the verge to conserve the environment and abide by the global regulations on environmental conservation, natural fibers are gaining popularity [4,21]. Many researchers have investigated the root causes and contributing factors for the fogging phenomenon, with little evidence being found on the primary reasons for fogging on biocomposites.

Howick [35] investigated the causes of fogging in the automotive Plasticized-Polyvinyl Chloride (P-PVC) windscreen using three separate windscreen samples. In his study, he identified that amines were present in all three samples and suggested a link between fogging and these substances (Howick [35]). However, minimal research has been done to reduce the VOCs emissions from biocomposites [49]. Chen et al. and Kim et al. [3,50] investigated the acoustic and fogging properties of the polymer reinforced with natural nonwoven fiber. For instance, Chen et al. [3] reinforced the PP with the 50%wt. spunlaced flax nonwoven fiber using the hot press process for the automotive interior application. Based on the G method of the Fogging test, it was observed that the impurity of the flax fiber was removed during the spunlacing process. However, it increased the surface area of the nonwoven web, which resulted in increasing the fogging precipitation. Kim et al. [50] characterized the physical properties of the kenaf nonwoven fiber mixed with low melt polyethylene terephthalate (LM PET) and PP specimens manufactured with different processing conditions. It was noticed that specimens with a large amount of LM PET and high needle depth produced high tearing and tensile strengths. In addition, the gravimetric fogging test method showed that larger pore size allowed the easy flow of the VOCs gases, which aids in reducing the fogging values.

In an attempt to dig deeper into the emission of VOCs from biocomposites, Kim et al. [36,37,51,52] incorporated inorganic fillers as a scavenger to capture the VOCs. The inorganic fillers are crystalline inorganic materials with a high SiO2 to Al2O3 ratio. The filers have a three-dimensional network of the large pore, with a high ability to absorb water [52,53]. Therefore, the inorganic fillers were used in the experiment because they were expected to absorb VOCs [52,53]. The study by Kim et al. [36,37,51,52] established that VOC emission levels in biocomposites were considerably high, justifying the need to embrace sustainable materials, particularly natural fibers, for processing used to manufacture automobiles and other widely used construction materials.

Kim et al. [36] also studied the different percentages of volcanic pozzolan in reducing the odor and VOCs from the polypropylene (PP) filled with wood fiber (WF) and rice husk fiber (RHF). This study demonstrated that increasing the volcanic pozzolan to 3%wt. slightly decreases the tensile and flexural properties of the composite (Kim et al. [36]). Furthermore, it was found in the research that at 1% wt. volcanic pozzolan, the toluene emission was 44 ppb in PP-RHF, and at 3%wt., toluene emissions were at 27ppb in PP-WF (Kim et al. [36]). From this study, it can be concluded that the optimum content of the volcanic pozzolan is 1%wt. without affecting the mechanical properties of the biocomposites.

Kim et al. [37] further replicated the experiment done in Kim et al. [36], but this time with polybutylene succinate (PBS), polylactic acid (PLA), bamboo flour, and wood fiber included in the biocomposites. This study found that adding the 3%wt. of the natural zeolite and synthetic zeolite decreases the emission of the VOC (Kim et al. [37]). This finding is explained through the fact that inorganic fillers have pore structures that can absorb the oxidation and the thermal degradation gases of the natural flour and matrix, leading to a significant reduction in the VOCs emission. It is also essential to note the finding of the study by Kim et al. [38], which showed that

adding the inorganic filler storage modulus led to a reduced VOCs emission, the glass transition temperature (Tg) for the biocomposite remained unchanged.

Kim et al. [49] went ahead to do another study using natural zeolite and synthetic zeolite to determine their impact on VOCs emissions. Based on the analysis of the experiment's results for this research, Kim et al. [49] established that at 3% wt., the VOCs emission was decreased while enhancing the thermal stability of the biocomposites filled with wood fiber (WF) and rice husk fiber (RHF). A deeper analysis of the study's results established that the mechanical properties of the biocomposite showed that 3% wt. of the natural and synthetic zeolite is the optimum level since it did not impact the tensile and flexural strengths of the biocomposite.

Kim et al. [52], went on to complete yet another study that sought to use the volcanic pozzolan to reduce the total VOCs and formaldehyde emissions from the medium density fiberboard (MDF) furniture application. This study found that at 1% wt. and 3% wt. the total VOCs and formaldehyde emissions were reduced without compromising the mechanical strength of the biocomposite. Thus, it is justified to deduce from this finding that 1%wt. and 3% wt. are the optimum levels of volcanic pozzolan adaptable to reduce the total VOCs and formaldehyde emissions from the MDF furniture. Moreover, the study found that at 1%wt. of the pozzolan, the bending strength of the MDF furniture increased significantly (Kim et al. [52]). Nevertheless, the study affirmed that the increase in pozzolan content did not considerably increase the bending strength of MDF furniture because of the interfacial failure between hydrophilic and hydrophobic materials used for manufacturing the furniture Kim et al. [52]. Therefore, the study confirmed the anticipated outcome for the experiment by showing that the increase in the pozzolan content leads to the decline in the formaldehyde and total VOC emission from the MDF furniture since pozzolan is made of a porous structure that captures and absorbs the VOC emissions.

Table 3. Summary of the past studies done to reduce the fogging and VOCs in the biocomposites

Matrix	Fiber and filler content	Goal	Tests	Application	Ref.
PP	50%wt. spunlaced flax nonwoven fiber	Investigate acoustical and fogging performance	Acoustical properties test and G method of the fogging test	Auto-interior parts	[3]
PP, and PP/MAPP	30% wt. wood flour and rice husk flour; 0.5, 1, and 3%wt. volcanic pozzolan	Reduce the VOCs emission and odor	Tensile, Izod impact test, three-point bend test, GC-MSD analysis, and SEM/EDX analysis	Interior materials for automotive and building	[36]
PBS and PLA	3% wt. inorganic fillers such as pozzolan, white clay, natural and synthetic zeo, 30% wt. bamboo flour, and wood flour	Reduce the VOCs emission	Tensile and three-point bend test, DMA using dual cantilever method, TMA to measure the thermal expansion, GC-MSD analysis	Structural application in automotive and building industries	[37]
LM PET and PP	30 and 40%wt. kenaf nonwoven fiber	Examine the physical properties	Tensile and tearing strengths, G method of the fogging test	Automotive	[50]
PP	1, 3, and 5%wt. natural and synthetic zeo; 30% wt. wood flour and rice husk flour	Reduce the VOCs emission and odor	Mechanical testing including tensile and three-point bend test, TGA, GC-MSD	Interior materials for automotive and building	[51]
UF resin and ammonium chloride	1, 3, 5, and 10% wt. volcanic pozzolan, pine flour	Reduce formaldehyde and total VOC (TVOC) emission	formaldehyde emission test, bending strength, and internal bonding test	Furniture	[52]

On the other hand, many researchers have investigated the creep behavior and thermal analysis of biocomposites, mainly aiming at examining the long-term durability of naturally filled composites. For example, Siregar *et al.* [54] examined the thermal properties of the high impact

polystyrene (HIPS) reinforced with pineapple leaf fiber (PALF) without or with compatibilising agents such as polystyrene-block-poly(ethylene-ran-butylene)-block-poly(styrene-graft- maleic anhydride), and poly(styrene-co-maleic anhydride). TGA analysis indicated that HIPS reinforced with the PALF enhanced the thermal decomposition of the composites. The addition of the polystyrene-block-poly(ethylene-ran-butylene)-block-poly (styrene-graft- maleic anhydride) as compatibilizers and PALF treated with alkaline slightly improved the decomposition of the composites. However, poly (styrene-co-maleic anhydride) reduced the thermal decomposition of the composites.

On the other hand, Kaymkci *et al.* [55] investigated the effects of zeolite and MAPP on the physical, mechanical, and thermal properties of PP reinforced with pine flour. Increasing the zeolite content from 10 to 50% decreased the flexural and tensile properties due to the weak interfacial adhesion between PP matrix, wood flour, and zeolite. In addition, the TGA test indicated the thermal stability of the pine four/PP enhanced with the increasing zeolite because of the silicate presents in the surface region of the zeolite. Therefore, according to the test performed in this study, the optimum content should be 40/10/50/3 for the pine flour/zeolite/PP/MAPP to achieve satisfactory results.

Mengeloglu *et al*. [56] examined the thermal degradation of the thermoplastics such as recycled PP and recycled high-density polyethylene (HDPE) filled with recycled wheat straw flour (WF). They also examined the effect of maleated polyolefins such as MAPP and maleated anhydride grafted polyethylene (MAPE) as a coupling agent on the mechanical properties of the composites. TGA test indicated that adding the WF diminished the degradation temperature of the composites. Also, the poor adhesion between the wheat straw flours and the polymer matrix of the composites without the coupling agent was observed under the SEM. However, composites with

the coupling agents showed good compatibility between WFs and thermoplastics. Additionally, the mechanical properties of the HPDE and PP-based composites produced similar tensile and flexural results.

Hosseinihashemi *et al*. [57] studied the thermal stability of the PP-based composites as an effect of the almond shell flour (ASF) and montmorillonite nanoclay (MNT). TGA analysis showed that the thermal stability of the PP diminished due to the ASF; however, when the MNT was added to the composites, thermal stability and degradation temperature enhanced. Furthermore, it was observed under the SEM that composites without the MNT exhibited the ASF separation from the matrix and ASF agglomeration. With the addition of the MNT, less separation and agglomeration of ASF was observed, which proved that MNT was effective in improving the interaction of the ASF with the polymer matrix.

Thermal degradation of the PP reinforced with various natural fibers such as wood flour, rice hulls, newsprint, and kenaf fibers was examined by Tajvidi *et al*. [58]. SEM analysis showed the fiber pull-outs from the fractured surfaces of the samples without the MAPP. Nevertheless, MAPP proved to be effective in enhancing the fiber/matrix interaction as no fiber pull-out was observed from the fractured surfaces of the samples with the MAPP. TGA analysis showed that PP reinforced with rice hulls was least thermally stable, and it exhibited a high residual mass due to their high ash content. However, MAPP slightly reduced the thermal stability of the composites

For another instance, Tajvidi *et al*. [45] estimated the short and long-term creep behavior of the wheat straw polypropylene composites at a temperature range of 50-90°C. The experiment in the study by Tajvidi *et al*. [45] established that biocomposites have low creep resistance. The study further established that with the addition of the natural filler, the creep behavior of the wheat straw composites was enhanced considerably (Tajvidi *et al*. [45]). In the same vein, research

conducted by Xu *et al*. [59] investigated the creep behavior of the polyvinyl chloride (PVC)/bagasse fiber, bagasse fiber/ high-density polyethylene (HDPE), and HDPE with commercial wood at different temperatures. This study was designed to observe the impact of temperature on the creep behavior of biocomposites. According to Xu *et al*. [59], it was found that temperature is a critical parameter in the creep behavior of biocomposites. Principally, the study found that an increase in temperature causes increased stress in the materials over time, leading to enhanced creep behavior in the materials.

Other researchers have investigated the influence that temperature has on the creep behavior of biocomposites. A notable study is by Amiri *et al*. [8], which characterized the long-term behavior of flax/ vinyl ester composites at temperature ranges of between 30℃ and 110℃ using the time-temperature superposition (TTS) behavior. In the experiment conducted in the study, the master curve was plotted by shifting the creep compliance data to a reference temperature of 30℃ (Amiri *et al*. [8]). The study concluded that TTS is a valuable and accurate method to predict the long-term behavior of biobased composites (Amiri *et al*. [8]).

Amiri *et al*. [13] further performed a similar study on the alkaline treated flax fibers by adding 1% acrylic resin to vinyl ester. From this experiment, Amiri *et al*. [13] established that the creep compliance results exhibited a delay and consequential decline in the creep response due to 1% acrylic resin to vinyl ester and alkaline treatment of flax fiber. Hence, it is inferable from this experiment that the addition of acrylic resin to vinyl ester increases the alkalinity of the biocomposite, which in turn decreases the creep response of the flax fiber.

In another experiment, Amiri *et al.* [60] sought to investigate the mechanical and thermal behavior of the methacrylate epoxidized sucrose soyate (MESS) resin reinforced with flax fibers. The experiment showed that vertical and horizontal shift factors produced a smoother master curve

for loss modulus and storage modulus than creep strain curves obtained from the horizontal curve factor Amiri *et al.* [60]. In contrast, the study found that the creep strain master curve was achievable from only the horizontal curve factor (Amiri *et al.* [60]). Furthermore, when the Findley and nutting model was compared with the actual experimental creep data, the nutting model had a better agreement with the experimental data than the Findley model. This finding proves that the reinforcement of MESS resin with flax fibers significantly impacts the thermal behavior and creep behavior of biocomposites.

In a different experiment, Pérez *et al*. [61] evaluated the fracture surface of the modified and unmodified PP reinforced with the red pine flour. This experiment showed that the addition of the wood flour to the PP increased the biocomposite's modulus (Pérez *et al*. [61]). However, the study found that adding wood flour to the PP resulted in a significant decline in the tensile strength and fracture toughness of the biocomposite (Pérez *et al*. [61]). The study further established that adding MAPP enhanced the tensile strength of the biocomposite but did not significantly change the toughness of the biocomposite (Pérez *et al*. [61]). Generally, this experiment affirmed that the fiber pull-out and debonding were the primary failure mechanism observed in the unmodified composites under the SEM. The modified composites had better interfacial adhesion, which improved the tensile and fracture properties of the biocomposites. Therefore, it is deducible from the findings of this experiment that the addition of MAPP in the raw materials for manufacturing biocomposites has desirable outcomes, with a notable one among many being an enhanced adhesion effect on the particles, which consequently improves the biocomposite's tensile and fracture properties.

In yet another experiment on biocomposites, Chui et al. [62] analyzed the interface compatibility between wood flour and PP using coupling agents like MAPP and maleic anhydride

grafted ethylene-propylene-diene copolymer (MA-EPDM). SEM images showed that MAPP and MAEPDM enhanced the dispersion and interfacial adhesion of the wood flour and the compatibility between flour and polymer matrix (Chui *et al.* [62]). However, whereas the study found that the loss factor of the modified composites decreased, it proved that the MAPP was more effective in improving the interface compatibility of the biocomposite than the MAEPDM was. Hence, it can be concluded from this experiment that manufacturers of plastics should consider reinforcing their raw materials with the MAPP rather than MAEPDM to achieve enhanced outcomes in terms of environmental conservation.

Table 4. Summary of the past studies done on thermal analysis, creep behavior, and morphology of the biocomposites

Matrix	**Fiber and filler content**	**Goal**	**Tests**	**Application**	**Ref.**
Vinyl ester resin, 1% acrylic resin	Untreated and alkaline treated flax fiber	Study the long-term creep behavior and mechanical properties	Mechanical test and creep test in flexural bending mode	Structural application	[8]
Vinyl ester	Flax fiber	Modeling long term creep behavior	creep test in flexural bending mode	Structural application	[13]
PP	15 and 30% wt. wheat straw; 15 and 30%wt. of various mineral fillers	Study the creep behavior	Short-term creep test using single cantilever mode	Hood applications in the auto industry	[45]
HDPE and HDPE/MAPP	50% wt. kenaf fiber	Predict creep behavior	Frequency sweeps and creep test in dual cantilever mode	Structural building products	[46]
HIPS and/or coupling agents	50%wt. pineapple leaf fiber	Study the thermal behavior	TGA and DSC	–	[54]
Recycled HDPE and PP	50%wt. wheat straw flour	Evaluate the thermal behavior	TGA, DSC, SEM, tensile, and flexural test	Lumber decking boards	[56]

Table 4. Summary of the past studies done on thermal analysis, creep behavior, and morphology of the biocomposites (continued)

Matrix	**Fiber and filler content**	**Goal**	**Tests**	**Application**	**Ref.**
PP/ 2%wt. MAPP	30,35,40%wt. almond shell flour; 2.5 and 5.0%wt. montmorillonite nanoclay	Study the thermal stability	TGA and SEM	–	[57]
PP and or 2%wt. MAPP	50%wt. various natural fiber	Investigate the thermal degradation	TGA, DSC, and SEM	–	[58]
RPVC, VPVC, RHDPE, and VHDPE	Various %wt. of bagasse fiber	Characterize the creep properties	creep test using a dual-cantilever mode	–	[59]
MESS resin	Flax fiber	Study the thermal behavior	creep test using a dual-cantilever mode	Structural application	[60]
PP/MAPP	10,20, and 30%wt. pine fiber	Analyze the fracture surface	SEM and mechanical characterization	Structural application	[61]
PP/MAPP/ MA-EPDM	40%wt. wood flour	Analyze the interface compatibility	Dynamic mechanical analysis (DMA) using a three-point bending and SEM	–	[62]
PP/MAPP	10-50%wt. pine flour, 10-50%wt. zeolite	Investigate physical, mechanical, and thermal properties	Tensile and flexural properties, TGA, and DSC	–	[55]

3. OBJECTIVES

Polypropylene (PP) has an excellent cost-performance ratio and materials properties. It is a widely used polymer in automotive, mechanical engineering, and electronics [2]. However, automotive recycling composites are complex as those are made from petrol-based polymers [3]. As a result, the automotive industry are incorporating more bio-based materials due to the environmental and regulatory requirements [4,21]. Natural fibers bring challenges such as weather and thermal degradation and Volatiles Organic Compounds (VOCs) emissions during the degradation [15,49,63]. Creep behavior was investigated to identify the durability of biocomposites.

In summary, the main objectives of this study are:

- The main objective of the proposed study is to lessen the fogging effect using porous fillers to target responsible constituents.
- Another objective of this study is to develop long-term behavior prediction models to be used by researchers and engineers in industries working with bio-based plastics

4. MATERIALS AND METHOD

The fiber used in this study was flax fiber, wood fiber such as maple, and pine flour provided by RheTech (Whitmore Lake, MI, USA). For the matrix, Polypropylene copolymer (PP) was obtained from RheTech with a melt mass flow rate of 20g/10min and specific gravity of 0.9. Based on the SEM Images, the flax fiber length and diameter was approximated to be between 60-70µm and 45-55µm respectively. The maple fiber length and diameter were interrupted to be 10-30µm and 6-8µm and the pine fiber length and diameter was 40-50µm and 60-70µm respectively.

Table 5. Chemical constituent of natural fibers used in this study

Fibers	Cellulose	Hemicellulose	Lignin	Ash	Crude Protein	Nitrogen	Fat
Flax	85.10	6.89	2.78	1.16	2.68	0.43	0.61
Maple	59.49	22.31	14.60	0.48	0.49	0.08	0.00
Pine	49.30	16.86	25.37	0.33	0.39	0.06	1.19

Note: values are in percentages.

Table 5 represents the chemical constituent analysis done by the previous lab group members during the preliminary stage of this work on the fibers used in this study. These chemical constituents are in the similar ranges mentioned by the others [11,63,64]. The sum of the chemical composition of the porous fillers should be added up to approximately 100%. In the synthetic zeolite, the total is around 94%; it is because some of the content gets removed during the synthesis process of the natural zeolite.

Table 6. Chemical composition of the porous fillers

Element	SiO_2	AI_2O_3	TiO_2	Fe_2O_3	MgO	CaO	Na_2O	K_2O	MnO	P_2O_5	Sum
SZ	54.5	2.20	0.20	1.4	28.9	3.5	-	3.60	0.02	0.10	94.42
NZ	66.7	16.2	0.40	3.90	1.90	4.4	1.80	3.42	0.03	0.10	98.85
VP	76.2	13.5	0.20	1.10	0.05	0.2	1.60	1.80	0.10	5.00	99.75
WC	52.0	45.0	0.80	0.40	0.00	0.6	0.05	0.10	0.03	0.10	99.08

Note: units are in %.

Natural zeolite (NZ) was obtained from KMI Zeolite Inc (NV, USA), and synthetic zeolite (SZ) was acquired from Zeochem (OH, USA). Volcanic pozzolan (VP) was acquired from Hess Pumice Products, Inc (ID, USA) and white clay (WS) from Inner Mongolia Rational Industry Limited (Inner Mongolia, CN). The chemical composition of each porous filler used in this study is mentioned in Table 6 above. These chemical compositions were obtained from the vendors from where the porous fillers were purchased. The porous filler mentioned natural zeolite, synthetic zeolite, volcanic pozzolan, and white clay had a particle size of 7-10μm and were in very fine powdered form. Figure 5 shows the types of natural fibers and inorganic filler used in this study.

Figure 5. (a) Porous filler, and (b) flax, (c) pine (d) maple fiber

4.1. Material Processing

All materials were compounded in a co-rotating Leistritz (Micro18-GL) dual-screw extruder (Figure 6. a) with a temperature profile from feed throat to the nozzle in 148.9, 157.2, 160, 162.8, 165.6, 168.3, and 173.9, and 173.9℃, respectively. Screw speed is 150rpm at approximately 1.4MPa of backpressure in the barrel at the die. PP, fibers, and porous filler were dried in a convection oven (Model 1370FM, VWR) at 80℃ for 24hrs. before extrusions. The loading for all fibers was 20% fiber-77% polypropylene and 3% porous filler. Once the materials were oven-dried, the desired quantities were placed in the Ziploc baggy and mixed homogeneously by gently shaking the Ziploc baggy.

Once in a while, using the flexural beam as a spatula, the wood flour such as maple or pine flour and polymer were mixed in the feed hopper to ensure the even dispersion of the wood flour in the polymer during the extrusion. Since the flax fiber was long fibers, it was manually fed at the throat. To assure that set flax fiber loading was added to the throat, small cups were filled with 40g of PP/additives and 20% flax fiber which was 8 grams of flax fibers measured and rolled into small balls. Simultaneously PP/additives and flax fibers were fed at the throat of the extrusion. Next, materials were extruded through a water-cooling bath as long strands of the reinforced polymers. Finally, it was fed into the cutter attached to the extrusion to make the 2.5 to 3mm diameter pellets. Table 7 shows the description of the material processing and their IDs.

Table 7. The material processed in this study

No.	Description	ID
1	PP/Synthetic zeo	PSZ
2	PP/Natural zeo	PNZ
3	PP/Volcanic pozzolan	PVP
4	PP/White clay	PWC
5	PP/Maple Fiber	20% Maple
6	PP/MF/Synthetic zeo	PMSZ
7	PP/MF/Natural zeo	PMNZ
8	PP/MF/Volcanic pozzolan	PMVP
9	PP/MF/White clay	PMWC
10	PP/Pine Fiber	20% Pine
11	PP/PF/Synthetic zeo	PPSZ
12	PP/PF/Natural zeo	PPNZ
13	PP/PF/Volcanic pozzolan	PPVP
14	PP/PF/White clay	PPWC
15	PP/Flax Fiber	20% Flax
16	PP/FF/Synthetic zeo	PFSZ
17	PP/FF/Natural zeo	PFNZ
18	PP/FF/Volcanic pozzolan	PFVP
19	PP/FF/White clay	PFWC

Before injection molding, the pellets with porous media were dried in a convection oven for 24 hours at 80℃. Then, materials were injection molded using Maruka FCS (Model FA-100SV) injection molded (Figure 6. b) at barrel profile temperatures from feed throat to the nozzle in 171.1, 176.7, 182.2, 187.8, and 187.8℃, respectively for the PP/additives. A pressure of 3.4MPa and the velocity was 38.1mm/s was kept for injecting the material into the mold. The shot size for the flexural specimens was kept at 35.56mm, and the tensile specimens were kept at 38.10mm. For the PP/Fibers/additives, the barrel profile temperatures from the feed throat to the nozzle were kept at 168.3, 168.3, 171.1, 173.9, and 173.9℃ at the pressure of 3.45MPa and the velocity of 63.5mm/s. The shot size was 36.83mm for the flexural specimen, and for the tensile specimen, the shot size was 40.64mm.

Figure 6. (a) Leistritz Extrusion and (b) injection mold

Extruded pellets with porous filler milled using the Retsch Laboratory Mill, Figure 7(a) (Model SR300, Retsch® PA, USA) with a screen size of 0.75mm. Next, using the Carver, Figure 7(b) (Model 3856 Carver Inc., IN, USA), milled pellets were hot-pressed. First, the hot press was

turned to 190℃. Next, all surfaces of the mold were coated with the three layers of the FreKote for the first plate of the day, and later the surfaces were coated with the one layer of the FreKote for the other plates. Once the surfaces were dried, put the mold together with the bolts and use the Allen wrench to tighten the bolts. Then measured the 33g of the materials and poured them into the mold. Finally, the materials were leveled in the mold using the clean popsicles sticks. Then, both parts of the mold were placed in the hot press separately and left the mold in the hot press for 30 minutes. After 30 minutes, both parts of the mold were taken out and placed on the cart wearing the proper heat-resistant gloves. The male part was placed on the bolted screwed tapped hole, and since it is tapered, it slid into the place very slowly.

The assembled mold was placed in the press again (Figure 7(c)). Again, the pressure up to 0.54MPa, was pumped with the increments for 30 seconds. Finally, the pressure was maintained at 0.54MPa for 10 minutes with the hot press was turned on. After 10 minutes, the hot press was turned off, and the mold was kept at that level for 10 more minutes while the fan was on. Once the pressure was decreased on the hot press, the mold was removed from the press and placed outside to cool down for another 45 minutes under the fan. After the mold was cool down, the plates (Figure 7(d)) were removed from the mold by unscrewing the bolts. The plates were handled with gloves hand and placed in the Ziploc baggy to maintain an environment of the least amount of contamination possible.

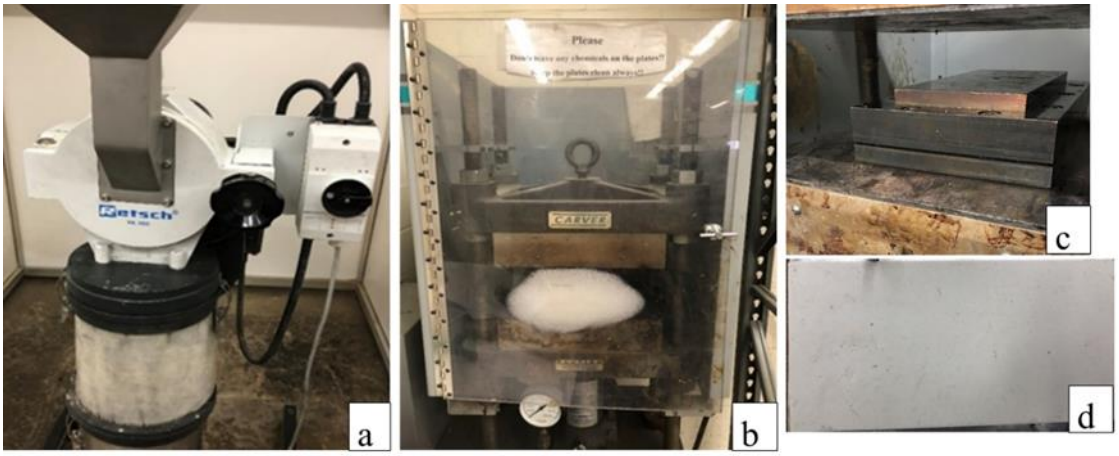

Figure 7. (a) Retsch Laboratory Mill, (b) hot press, (c) hot press mold, (d) hot-pressed plate

4.2. Mechanical Characterization

Mechanical properties are tested on the biobased composites with the natural porous media and without it. Tensile properties such as tensile strength and tensile modulus were performed using Instron Model 5567 (Instron® MA, US) as per ASTM D638 using a 5mm/min crosshead rate [65]. Five specimens were prepared in the dog-boned (dumbbell-shaped) according to ASTM D638 and tested for each test sample. The overall sample size of the injected specimen was $165(\pm 3)mm\ (L) \times\ 19(\pm 2)mm\ (w) \times\ 3(\pm 0.5)mm\ (t)$. Before performing the tensile test for the day, the load frame was calibrated. The strain was measured with MTS extensometer model 632.25B-20 (Figure 8(a)), which was used to record the strain during the first portion of the testing. Once the specimen reached 1.5% elongation, the test was paused while the extensometer was removed. Testing then continued until the failure occurred or the load peaked. For each material set, five samples were tested, and then the average was taken.

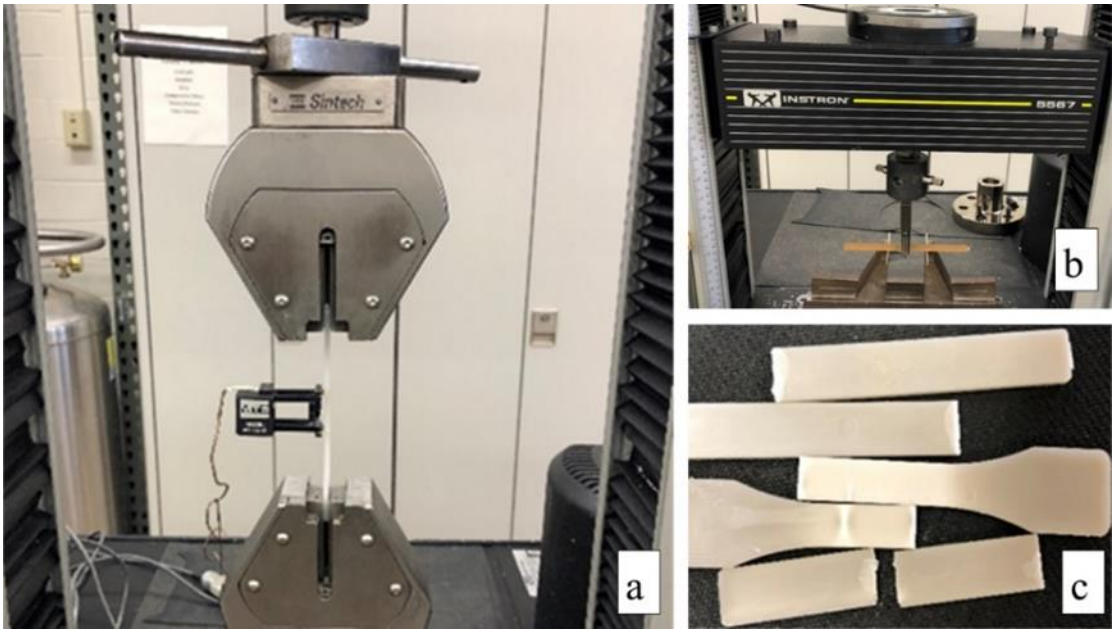

Figure 8. (a) Tensile Test Setup, (b) flexural test setup, and (c) fractured specimen

Flexural properties such as flexural strength and flexural modulus were measured through the three-point bend testing specified in ASTM D790 using Instron 5567 load frame Figure 8(b). For each material set, five samples were tested using the 3.2mm diameter loading and support pins. The injected flexural specimen size was $165(\pm 3)mm\ (L) \times\ 12(\pm 0.7)mm\ (w) \times\ 3(\pm 0.05)mm\ (t)$. The support span was kept at 16 times the means thickness of the sample set. The test rate was determined utilizing the following equation specified by the standard:

$$R\ =\ \frac{0.01\ L^2}{6d} \tag{5}$$

Where L is the support span and d is the sample thickness.

Impact test performed using Izod model 104 impact machine (Tinius Olsen, PA, USA) as per the ASTM D256 [66]. Flexural test specimens were marked mid-point for cutting in half under the wet saw for the impact test. After that, those prepared specimens were marked at mid-point to be notched (Figure 9(b)). The impact test was done with the additional weight as seen in the figure 9.b below. Five specimens are prepared in the rectangular cross-section for each material set and tested. Then the average of the five measurements is taken for the results.

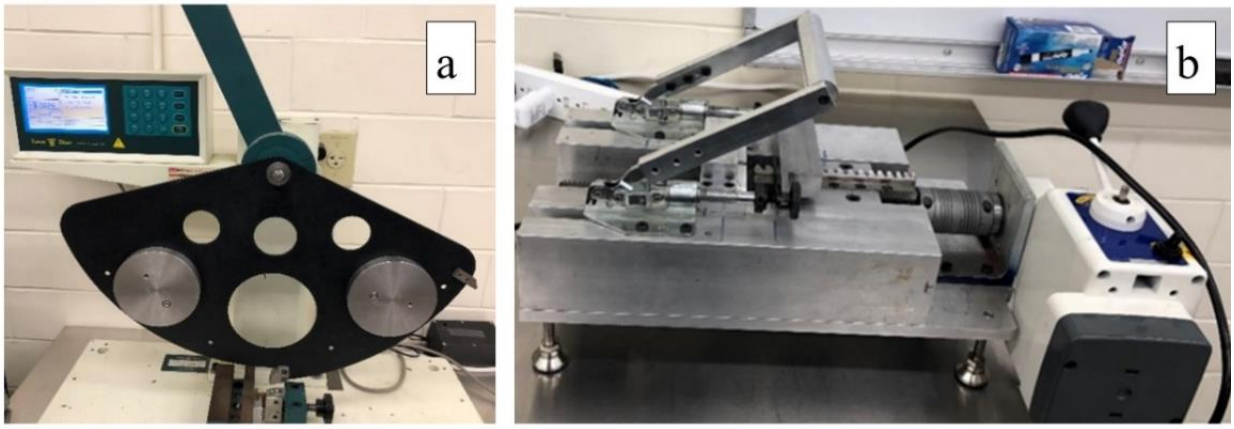

Figure 9. (a) Izod impact test and (b) notching machine

4.3. Creep Analysis

3-point bend test under the flexural mode was performed under the Dynamic Mechanical Analyzer (DMA) Q800 by TA Instruments (New Castle, DE, USA) for the creep behavior of the composites as per ASTM D5418 and ASTM D5023 [67,68]. Specimens were cut in the wet saw from the flexural test specimens with the dimension of $60(\pm 2)mm\ (L) \times\ 12(\pm 0.7)mm\ (w) \times\ 3(\pm 0.05)mm\ (t)$. After cutting the samples, they were oven dried at 80℃ until the moisture was removed. After that, they were kept in the Ziploc baggy until the testing. 3-point bend test ran under the isothermal creep test temperature ranging from 30℃ to 110℃ with increments of 10℃ by applying 10% of the maximum flexural strength of the sample set. However, for the neat PP, the creep test reached the strain capacity before 110℃; therefore, the data was only recorded up to 100℃ for the neat PP specimens. Each specimen was subjected to creep for 10 minutes and 10 minutes for recovery at each temperature step. Figure 10 shows the creep test set up in the DMA and bent test specimen due to creep.

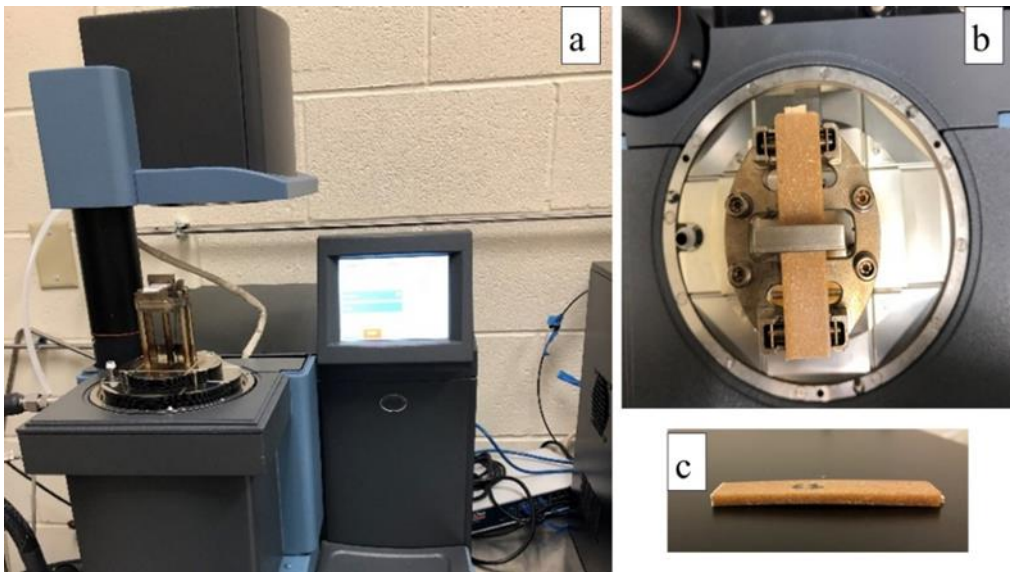

Figure 10. (a, b) Creep test set up and (c) test specimen after creep test

4.4. Thermal Analysis

Thermogravimetric Analysis (TGA) test carried out in TA Instruments Pyris™ 1 Thermogravimetric Analyzer equipment by PerkinElmer (MA, USA). The tests were performed from 25℃ to 450℃ with the increment of a 10℃/min ramp at an inert atmosphere. Around 3 ± 1 mg (Figure 11) of the specimen was cut from the extruded pellets per ASTM E1641-18 [69]. In addition, the percentage of weight loss over the temperate was recorded. The pan was balanced to remove the weight of the materials from the previous test, then waited until the weight on the computer screen was stabilized before putting the samples on the pan. After putting the samples on the alumni pan again, the load was balanced and waited for few seconds until the sample weight was stabilized before starting the test. The method was programed to hold the samples for 5 min. at 25℃ to stabilize the temperature from the previous test.

Figure 11. (a, b) TGA test set up (c) samples for the TGA test

4.5. Fogging Test

Fogging characteristics of the thermoplastics filled with natural fiber and porous filler determined as per method F and method G mentioned in ISO 6452 standard [70]. In the hole saw, circular test pieces with 80 ± 1mm diameter from the composite plate made in the hot press (Figure 7) were cut using the Hole Dozer™ (Milwaukee, WI, USA) and specimen cutting jig (Figure 12). Before cutting the specimens, specimen cutting jig and hole saw were cleaned with acetone to avoid contamination during the cutting of fogging specimens.

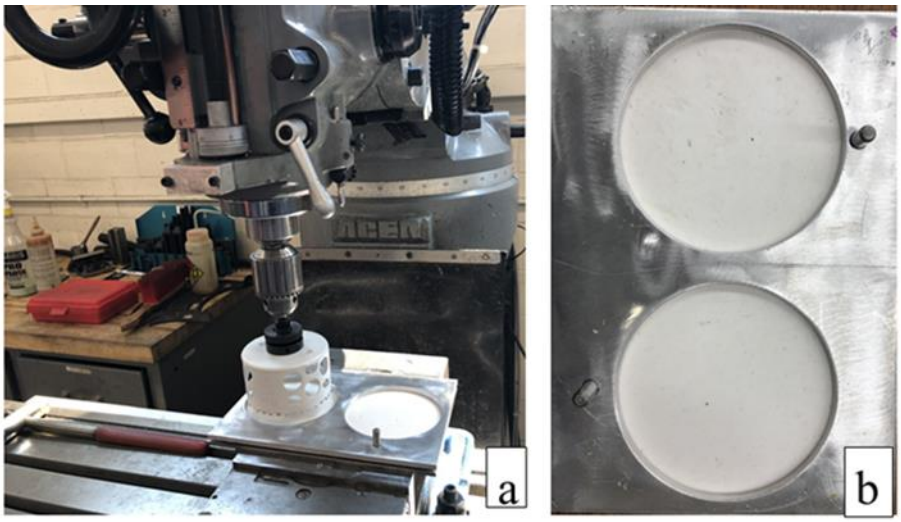

Figure 12. (a) Hole saw and (b) specimen cutting jig

Container (Presto Model # 01781 23-Quart Pressure Canner) was filled with mineral oil was placed on the hot plate (Figure 13) to create the oil bath for the fogging test. The mineral oil level was kept at 60mm from the lower surface of the glass plate placed on the beaker. The temperature of the hot plate was set at 100℃. However, the temperature fluctuated between 100℃ to 105℃. A magnetic stirrer was placed in the oil container and kept at 100rpm to maintain the slow agitation of the fluid. It was required to put the beaker in the oil bath when the oil bath temperature reached 100℃. Therefore, to heat the oil faster for the first test of the day, water immersion was placed inside the oil container was kept on until the oil bath temperature reached 100℃. Then, water immersion was turned on again for few seconds to avoid the oil bath temperature dropping more than 5℃ for more than 20 minutes. Prior to testing the specimen for the F method (Reflectometric method), samples were put in the desiccator for at least 16hrs. at 23℃ and 45% relative humidity. However, in the standard, it was mentioned to condition the samples at 50% relative humidity. Once conditioned, they were put in the clean beakers, covered with the glass plate, and sealed with the sealing rings, followed by the filter paper and cooling plates for the testing (Figure 13).

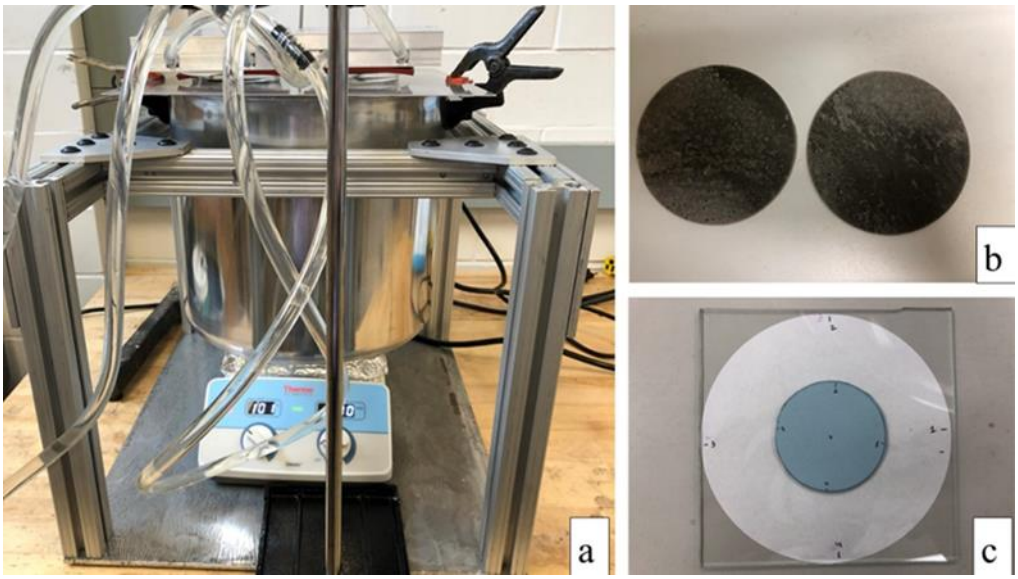

Figure 13. (a) F method test set up (b) test specimen (c) glass plate with spacer

The filter paper was placed to avoid scratching the glass plates. Cooling plates were fabricated at the NDSU lab (Figure 14). A pump (Ironton® Submersible Pump, Model# P01-011-0012) was used and placed in the bucket to maintain the continuous flow of the cold water. The bucket cap was drilled with three holes; two holes to pass the tubing to the cooling plate and one for the tap water. Once the water temperature in the bucket got hot, the tap was turned on until the temperature reached 21℃. Then, another hole was drilled on the side of the bucket to allow the hot water to flow through. Before testing the specimens, beakers and glass plates were washed with non-alkaline detergent and rinsed with deionized (DI) water. Once they were cleaned, they were handled with gloved hands. Reflectometer reading using the Elcometer Model 480 (MI USA) was measured on the glass plates before and after putting in under the testing. The reflectometer values were measured at a distance of 25 ± 5 mm from the center of the glass plate at 90° apart from each reading. Four readings from R_{01} to R_{04} were taken. To ensure that the after-test readings R_{11} to R_{14} were taken at the exact location as R_{01} to R_{04}, spacers and the filter papers were marked with the location of each reading (Figure 13).

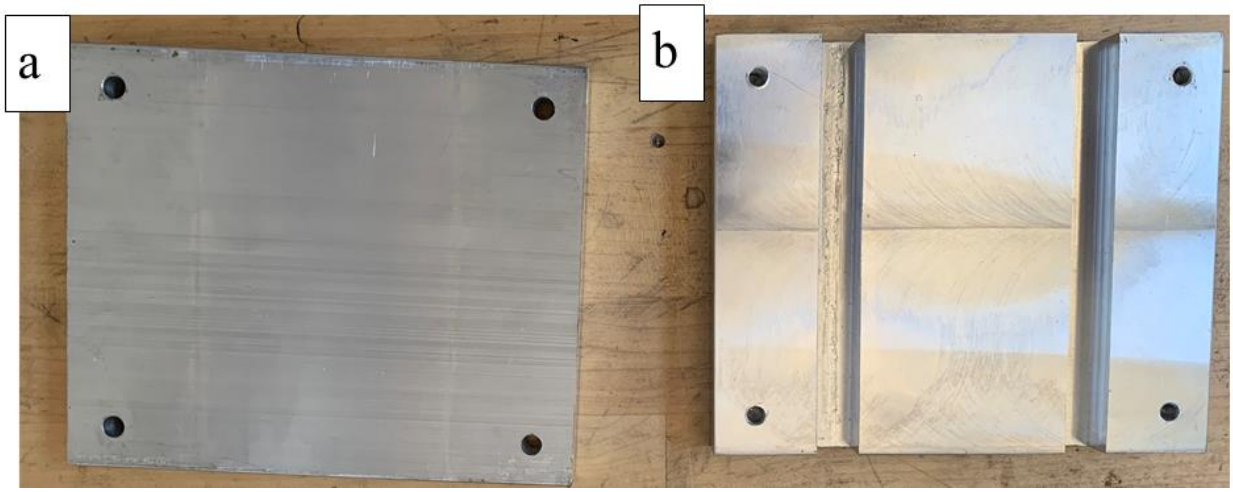

Figure 14. Cooling plate (a) top part and (b) bottom part

Once the R_{01} to R_{04} were taken, the glass plates R_0 values facing downward were placed on the sealing ring on the beaker; the prepared beakers were placed in the oil bath 180 ± 3 min at

the bath temperature of 100℃. The aluminum plate was drilled with the hole of beaker diameter; each hole was drilled at a minimum distance of 30mm apart. The distance from the wall of the container to the beaker was kept at 30mm. After the test was done, the fogged-up glass plates were stored in the desiccator with the fogging side up for 60 min at 23℃ and 45% relative humidity. The desiccator was placed in a way that direct sunlight does not come on the fogged-up glass plates. Then the R_{11} to R_{14} readings were taken as exact location as R_{01} to R_{04}. When taking the readings of the glass plates, the reflectometer was calibrated. The F value was calculated using the following equation.

$$F = \left(\frac{R_{11}}{R_{01}} + \frac{R_{12}}{R_{02}} + \frac{R_{13}}{R_{03}} + \frac{R_{14}}{R_{04}}\right) \times \frac{100}{4} \quad (6)$$

Where F is the fogging value for the plate in %, R_{01} to R_{04} are reflectometer readings before the fogged plate in %, and R_{11} to R_{14} are the reflectometer readings after the fogged plate in %.

Before testing the specimens for the G method (Gravimetric method), specimens were put in the desiccator for at least 16 hrs. at 23℃ and 45% relative humidity. Using the same approach as the F method (Figure 12), 80 ± 1 mm diameter of samples were prepared for the G method. In this method, aluminum foil (Figure 15(c)) was used to create a "Fog" that can be measured in the mass (mg). Firstly, the aluminum foil (Speedy-Foil®) was measured in the mg in the weighing scales. While handling the aluminum foil, a tweezer (Cole-Parmer Stainless Steel Tweezer # 7) was used to avoid touching the foil. When the foil was placed on the weighing scales, a paper wedge that came with the foil was placed on the weighing scale to keep the foil dust-free and getting contaminated, and then the scale was tare to zero. When the foil was taken to the next-door lab room for the measurements, it was wrapped in a clean paper towel to keep the foil as dust-free as possible.

After that, the foil was placed with the bright side facing downward on the sealing ring, followed by the glass plates on the loaded beaker (Figure 15). Then the assembled beaker was placed in the oil bath for 16 ± 0.1 hours, at the bath temperature of 103℃ (Figure 15). The hot plate temperature was set at 100℃; however, the thermostat in the oil bath was read as 103℃. A magnetic stirrer was placed in the oil container and kept at 100rpm to maintain the slow agitation of the fluid. As mentioned in the F method test, to heat the oil faster for the first test of the day, water immersion was placed inside the oil container was kept on until the oil bath temperature reached 100℃. Then, water immersion was turned on again for few seconds to avoid the oil bath temperature dropping more than 5℃ for more than 20 minutes. Since the G method was required to test for 16 hrs., a safety switch, as marked in the figure below, was assembled so the testing can be left unattended overnight without causing any hazardous conditions. When the test was left unattended, the camera was placed to monitor the temperature of the hot plate every 1-2hrs. During the unattended portion of the test, the tap was kept turned on at medium speed to avoid the cooling plates getting hot.

After the 16hrs of the oil bath, the fogged-up aluminum foils were stored in the desiccator with the fogging side up for 3.5hrs. at 23℃ and 45% relative humidity. The desiccator was placed in a way that direct sunlight does not come on the fogged-up foil. When the fogged-up foils were taken for the measurement, it was wrapped with the clean towels with the sealing rings on the foil to avoid touching the condensation fog and tweezer # 7 used to handle the fogged foil. The mass of the condensable constituents(G) was calculated using the below equation.

$$G = G_1 - G_0 \tag{7}$$

Where G is the mass of the condensable constituents on the disc in mg, G_0 is the mass of the discs before the test in mg, and G_1 is the mass of the disc after the test in mg.

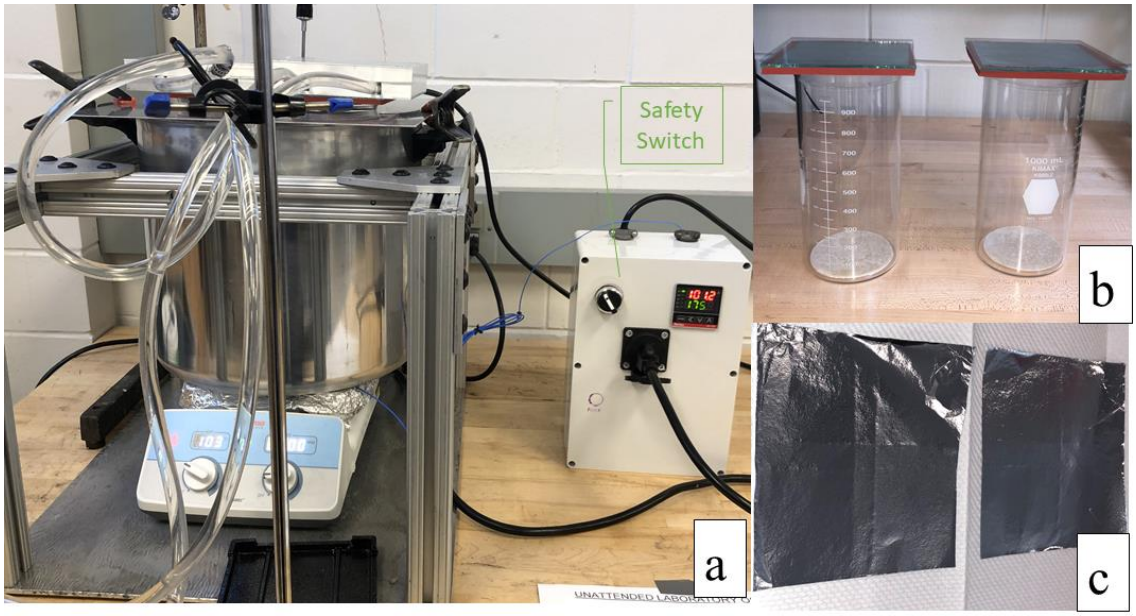

Figure 15. (a, b) G method test set up (c) aluminum foil pre-test

The equipment used in the Fogging test and the sources from where the equipment was ordered are listed in Table 8.

Table 8. List of equipment for the Fogging Test

Equipment/Material	**Specifications**	**Source**
Thermal-transfer fluid	Temperature stable and water-soluble (preferred fluid: polyhydric aliphatic alcohol)	Mills Fleet Farm
Glass-cleaning	Non-alkaline type	Menards
Thermostatically controlled bath	Designed to operate up to 130℃ (max difference allowed ±0.5℃)	Amazon (Presto)
Cooling plates	Hollow and made of corrosion-resistant metal; the side facing the glass plate made of aluminum; the mass of the cooling plates filled with water should be at least 1 kg	McMaster Carr (Fabricated as per ISO standard in NDSU Lab)
Flat-bottomed beakers	Dimensions as shown in ASTM E960	Supplymylab
Water pump	Ironton® Submersible Pump, Model# P01-011-0012	Northern Tools+Equipment
Sealing Ring	Silicon or fluoro rubber, L shaped or circular in cross-section, inner dia. 90mm to 95mm, thickness 2mm to 4mm, and hardness 50IRHD to 70IRHD	McMaster Carr (Fabricated the rings from rubber pad as per ISO in the NDSU Lab)
Float Glass plates	Residential or windshield window quality, thickness (3±0.2) mm, either square (110x110) mm or circular (dia. 103mm)	Lowe's
Filter paper	Diameter 110 mm and mass per unit surface area of 90g/m2	USA LAB

Table 8 List of equipment for the Fogging Test (continued)

Equipment/Material	Specifications	Source
Aluminum Foil Discs	thickness 0.03mm, diameter (103±1) mm	Sigma Aldrich
Reflectometer	With 60° incident beam and 60° measurement beam	Elcometer Inc
Spacer	Made from paper or plastic with a circular hole with the thickness (0.1±0.02) mm	Fabricated as per ISO standard in NDSU Lab
Dishwasher	Deionized-water supply	NDSU Chem Stockroom
Balance	Scale division of 0.1 mg	Fisher Scientific
Polyethylene gloves	No specification mentioned	McMaster Carr
Desiccator	No specification mentioned	Fisher Scientific
Lab Stand	No specification mentioned	Amazon
High-Temperature safety switch	No specification mentioned	Amazon (Fabricated as per requirements in the NDSU lab)

4.6. Image Analysis

Failed tensile specimens of the selected specimen were examined at the Electron Microscopy Center at NDSU. Scanning Electron Microscopy (SEM) images of the fractured surface of the biocomposites captured to investigate the particle size, dispersion of additives, fibers, and matrix interface of manufactured specimens under the A JEOL JSM-6490LV scanning electron microscope (JEOL, Peabody, Massachusetts, USA) at accelerating 15kV voltages. A summary of characterization methods, equipment, conditions, and standard test methods used in this study are presented in Table 9

Table 9. Summary of tests, equipment, and standards used in this study

Tests	Instrument	Conditions	Standard
Fogging	—	Method F and G	ISO 6452
GC-MSD	Agilent 5977A	—	—
Tensile Flexural	Instron 5567	W/ MTS extensometer 632.25B-20	ASTM D638 ASTM D790
Impact	Izod Impact	N/A	ASTM D256
Creep	DMA Q800, TA instruments	3- point bending	ASTM D5023 ASTM D5418
TGA	Pyris™ 1	25 °C to 450 °C (10 °C/min ramp)	ASTM E1641
SEM	JEOL JSM 6490LV	15 kV Voltage	—

5. RESULTS AND DISCUSSION

5.1. Mechanical Characterization

Figure 16 represents the tensile strength and tensile modulus. As seen from the graph that neat PP is producing the tensile strength on the average 24.74 (±) 0.48MPa and tensile modulus on the average of 1.72 (±) 0.12GPa, which is comparable to the study done in [33]. Stark *et al*. [33] reported the tensile strength of 28.5MPa and tensile modulus of 1.53GPa. In addition, neat PP samples are ductile, and during the constant tensile load, polymer chains start to break and lead to low tensile strength [71]. However, adding the volcanic pozzolan and white clay slightly decreased the tensile strength; it could be due to poor dispersion of the volcanic pozzolan and white clay in the polymer matrix [36]. Furthermore, neat PP with synthetic zeolite produces the highest tensile strength and tensile modulus on the average 27.36 (±) 0.64MPa and 2.56 (±) 0.87GPa, respectively. It's due to the lower organic content present in the synthetic zeolite.

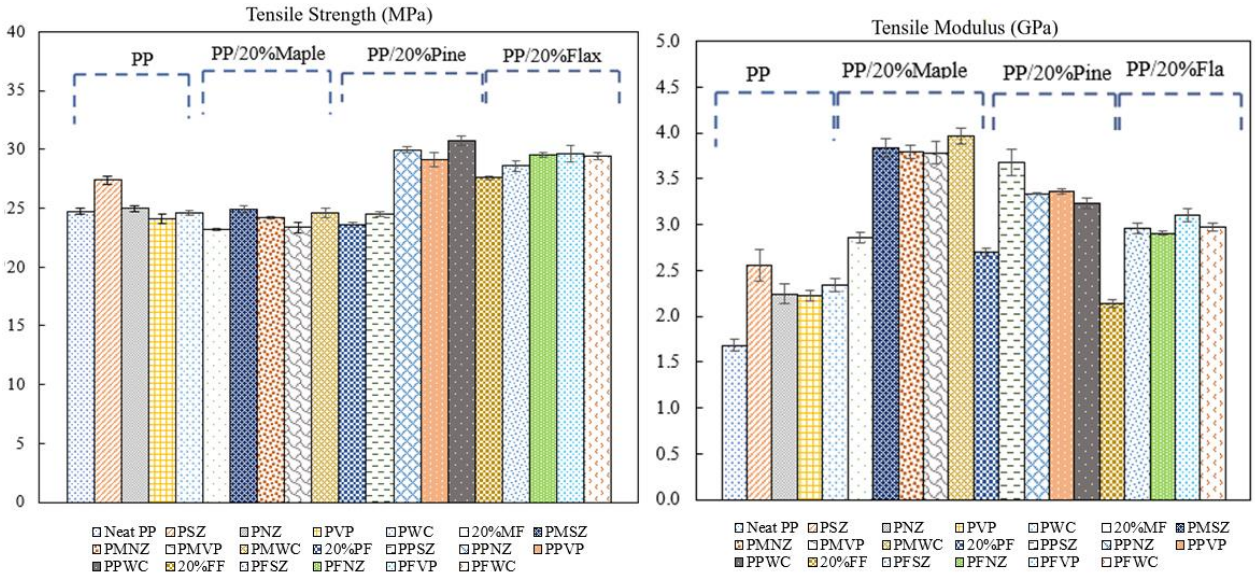

Figure 16. Tensile Strength (MPa) and Tensile Modulus (GPa) of the biobased composites

Also, adding the maple fiber into the PP enhanced the tensile modulus but slightly decreased tensile strength. Maple fiber with the PP exhibited a tensile strength of 23.20 (±)

0.25MPa, which is comparable to the study done in the past [30]. Kim *et al.* [30] reported the tensile strength around 24MPa of the composites reinforced with maple fiber. Maple fiber producing the low tensile strength is due to the high amount of hemicellulose present in the maple fibers compared to pine and flax. As mentioned previously, hemicellulose has an amorphous structure meaning molecules are not in uniform arrangement; therefore, it does not contribute to the load transfer during the tensile test [16,19]. On the contrary, adding maple fiber to the PP increased the tensile modulus of the composites. An increase in the tensile modulus with the addition of the maple fibers is due to the presence of cellulose in the maple, which contributes to the stiffness, thus increase the tensile modulus. Furthermore, adding the inorganic fillers did not significantly improve the tensile properties of the maple/PP composites. It is due to low compatibility and interfacial interaction between hydrophilic pozzolan and hydrophobic polymer matrix, which leads to the poor surface adhesion of the fiber and inorganic porous fillers [30].

Similarly, adding the pine fiber to the PP did not improve the tensile strength; however, it increased the tensile modulus of the composites. Pine/PP showed the tensile strength of 23.74 (±) 0.14MPa, which is comparable to the study done in the past [30]. Kim *et al.* [30] stated the tensile strength around 26MPa for the composites reinforced with the pine flour. As mentioned before, wood flour comprises three significant constituents: cellulose, hemicellulose, and lignin. In the pine flour, the amount of lignin is present is higher than the amount present in the flax fiber. Furthermore, the molecular structure of the lignin is amorphous [16,19]. Therefore, during the tensile test, it does not contribute to the load transfer thus produces low tensile strength. However, pine/PP improved the tensile modulus of the composites. Cellulose was also present in the pine fibers, which contributes to the stiffness, increasing the resistance to the deformation under the load. In addition, adding the inorganic porous fillers improved the tensile properties of the pine/PP

composites. Therefore, it can be inferred that there was no interfacial interaction between hydrophilic inorganic porous filler and hydrophobic matrix.

In this study, the inorganic porous filler with a particle size of 7-10μm was used. Since the particle size was very small. It was evenly dispersed in the polymer matrix and did not hinder the tensile properties. However, the image analysis was not performed to measure the particle size and shape since it does not give any insight into the effect of the porous fillers on the mechanical characterization of the composites. This was in a similar trend with the work done by Kim *et al.* [36,37,51]; in their study when the 3%wt. of porous fillers was added to the biocomposites and the wood flours. Again, no decrease in the tensile strength was observed.

PP filled with 20% flax fiber without additives produced a tensile strength of 27.60 (±) 0.29MPa, comparable to values reported by Garkhali *et al.* [23] and Van Den Oever [24] at 20% fiber loading. Garkhali *et al.* [23] and Van Den Oever [24] stated tensile strength value between 35 to 42MPa of the flax fiber reinforced PP. With the addition of the flax fiber, the tensile strength was increased as flax fiber has higher aspect ratios (fiber length to the diameter) and a higher amount of cellulose compared to the maple and pine flours, which helps in the load transfer during the tensile test. In addition, as mentioned before, cellulose has a crystalline molecule structure meaning the molecules are tightly arranged in order [16,19]. Also, adding the inorganic porous fillers to the flax/PP composites enhanced tensile properties. Therefore, it can be inferred that there was no interfacial interaction between hydrophilic inorganic porous filler and the hydrophobic matrix of the flax/PP composites.

Biocomposites filled with natural fibers and the additives did not significantly impact the flexural properties much, as shown in Figure 17. Net PP on average gave flexural strength of 47.44 (±) 1.23MPa and flexural modulus of 1.45 (±) 0.042GPa. As mentioned before, PP is ductile and

less rigid; therefore, it can resist bending while the point load is being applied to the specimen. Hence, it generates less flexural strength and flexural modulus. On the other hand, when the inorganic porous filler was added to the neat PP, the flexural properties were improved as those fillers make the PP more rigid. PP with synthetic zeolite was observed to produce high flexural strength and flexural modulus compared to natural zeolite, as synthetic zeolite has lower organic content present in the synthetic zeolite.

In contrast, adding the maple fiber improved flexural properties instead of the tensile properties. On average, the maple/PP produced the flexural strength of 51.93 (±) 2.69 MPa and flexural modulus of 2.22 (±) 0.071GPa. An increase in the flexural properties of the maple/PP composites due to the smaller particle size contributes to the stiffness and increases the rigidity of the composites; thus, it resists against the bending force. Also, adding the inorganic porous fillers, especially synthetic zeolite, increases the flexural properties as those inorganic fillers contributed to the stiffness. Moreover, some of the organic content gets removed during the zeolite synthesis process, thus giving the synthetic zeolite better dispersion than the natural zeolite.

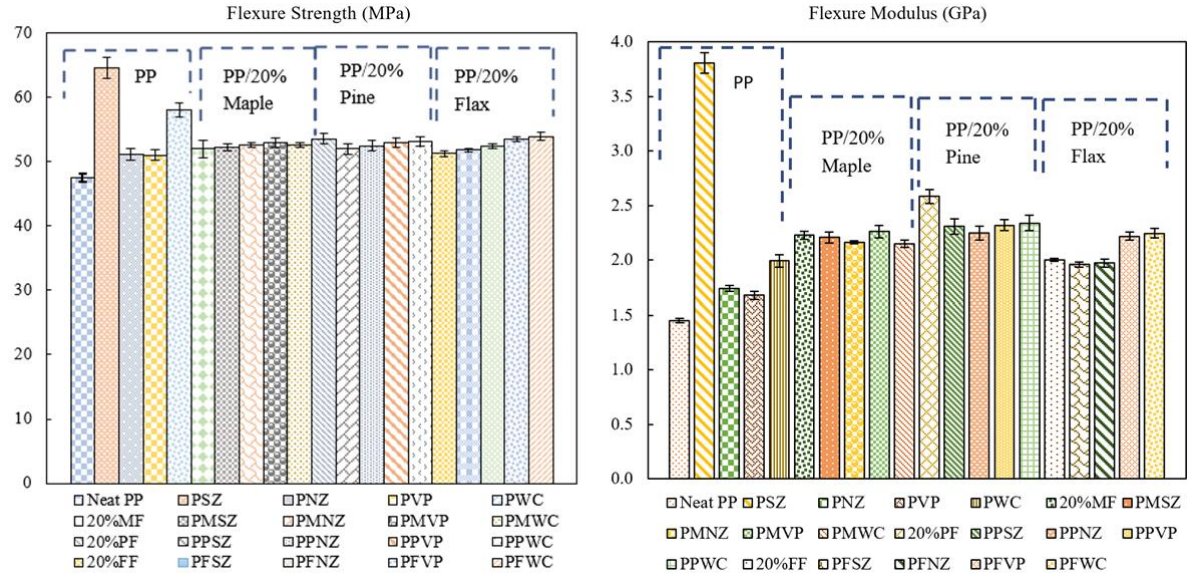

Figure 17. Flexural Strength (MPa) and Flexural modulus (GPa) of the biobased composites

Likewise, adding the pine flour to the PP composites had a similar pattern as the maple fiber. In addition, pine/PP exhibited flexural strength on the average 53.55 (±) 1.5 MPa and flexural modulus on the average 2.58 (±) 0.126 GPa. It can be noticed from the graph that pine fiber had higher flexural properties in comparison to maple fiber. Again, it has to do with the particle size difference. As pine fiber is finer than maple fiber; therefore, pine fiber has better dispersion and smaller agglomeration than maple fiber. Interestingly, when the inorganic filler was added to the pine/PP composites, it slightly decreased the flexural strength and flexural modulus. It could be due to the poor dispersion and agglomeration of the inorganic fillers in the polymer matrix, leading to poor flexural strength and flexural modulus.

Flax/PP exhibited the flexural strength on the average 51.25 (±) 0.915 MPa and flexural modulus on the average of 2.00 (±) 0.033 GPa, which was comparable to the study done by Van Den Oever *et al*. [24]. Furthermore, flax/PP had higher tensile strength and tensile modulus than the pine and maple; however, flax/PP had lower flexural strength and flexural modulus than the maple and pine composites. As mentioned before, flax fiber has higher aspect ratios (length to the diameter), which helped transfer the load during the tensile test. However, it did not contribute to the stiffness of the composites during the flexural test. Furthermore, adding the inorganic fillers slightly improved the flexural properties.

Izod impact strength of the polypropylene filled with natural fiber with different porous filler shown in Figure 18. The graph shows that neat PP has the lowest impact strength on the average of 2.46 (±) 0.533 kJ/m^2. Since the PP is ductile, it was observed during the impact test that crack propagation was initiated, and less energy was required to fracture the specimen. A similar pattern was observed in the Izod impact test as the tensile and flexural tests; adding the inorganic porous filler increased the impact strength. Inorganic porous fillers increasing the impact strength

of the PP was due to the porous fillers preventing the increase in the crack, thus requiring more energy to fracture the specimen [36]. In addition, PP with the synthetic zeolite has the highest impact strength compared to the other inorganic porous fillers. It could be due to the synthetic zeolite having a particle size of 7μm, which can lead to better dispersion and small agglomeration than the bigger particle size.

With the addition of the maple fiber, the impact strength was increased to 3.01 (±) 0.022 kJ/m^2 on average. The increase in the impact strength was due to the maple fiber increase the stiffness of the composites, so more energy was required for fracturing the samples. Additionally, adding the inorganic porous fillers improved the impact strength of the maple/PP composites. With the maple/PP composites, the volcanic pozzolan produced a higher impact strength than the white clay, synthetic zeolite, and natural zeolite. Whereas the synthetic zeolite with the maple and PP produced the higher tensile strength for the tensile test. It could be that volcanic pozzolan has a higher amount of silicon dioxide in crystalline form, which can suppress the cracks from growing further. Therefore, more energy was required for those samples to be fractured. Another reason for volcanic pozzolan to increase the impact strength could be that volcanic pozzolan has better compatibility with the maple fiber and PP matrix.

The pine/PP composites had a lower impact strength compared to the maple/PP fiber. Pine/PP produced an impact strength of 2.23 (±) 0.171 kJ/m^2. Pine fiber has a shorter length than maple fiber; therefore, more energy is needed to pull out the fiber from the matrix during the impact test. In addition, inorganic filler increased the impact strength of the pine/PP composites. The pine/PP/volcanic pozzolan had a higher impact strength than the white clay, synthetic zeolite, and natural zeolite. Again, it could be that volcanic pozzolan has a higher amount of silicon dioxide in crystalline form, which can suppress the cracks from growing further. Therefore, more energy

was required for those samples to be fractured. Another reason for volcanic pozzolan to increase the impact strength could be that volcanic pozzolan has better compatibility with the pine fiber and PP matrix.

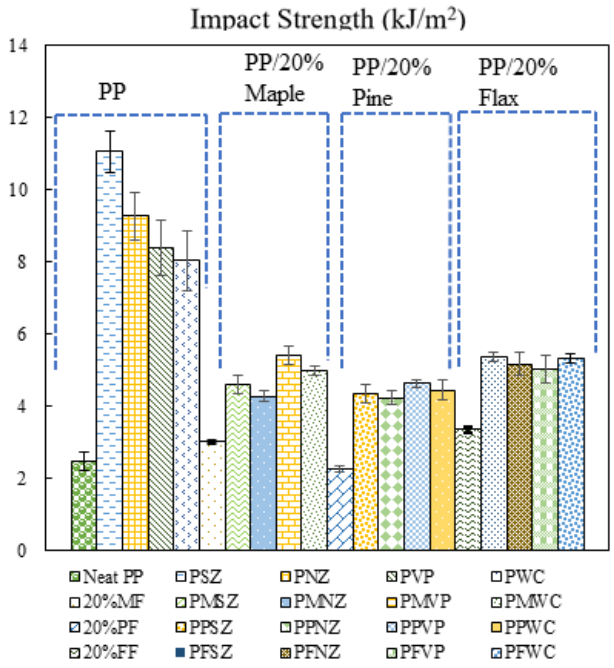

Figure 18. Impact Strength(kJ/m^2) of the biobased composites

In contrast, when flax fiber was added to the composites, it produces an impact strength on an average of 3.35 (±) 0.149 kJ/m^{2,} which was higher than the maple and pine fiber-based composites. Since flax fiber has a higher aspect ratio (fiber length to the diameter) compared to maple and pine, so it requires more energy to fracture the specimen with the long fiber compared to the short fiber. Furthermore, adding the inorganic porous fillers enhanced the impact strength of the flax/PP composites, especially synthetic zeolite. It could be that during the synthesis process, some of the organic matter gets removed, which improves the dispersion of the synthetic zeolite in the polymeric matrix. As mentioned before the impact test was performed with the additional weight and the fractured surface of the specimen was clean cut during the impact test. To get more

accurate impact strengths, the test needs to do without the weight and compared with the impact strengths due to the weight.

5.2. Creep Analysis

Creep tests at different temperatures from 30°C to 110°C were carried out on the composites reinforced with the natural fibers by applying 10% maximum flexural strength of the sample set. First in order to generate the master curve, the horizonal shift factors were calculated. Figure 19, shows the plotted graph of the Log (a_T) vs the T-T_0 (K) and using the polynomial 2nd order method the slope line was fitted through the data points for the neat PP and PP with natural fibers. This indicates that the shift factors are governed by the Williams-Landel-Ferry relations.

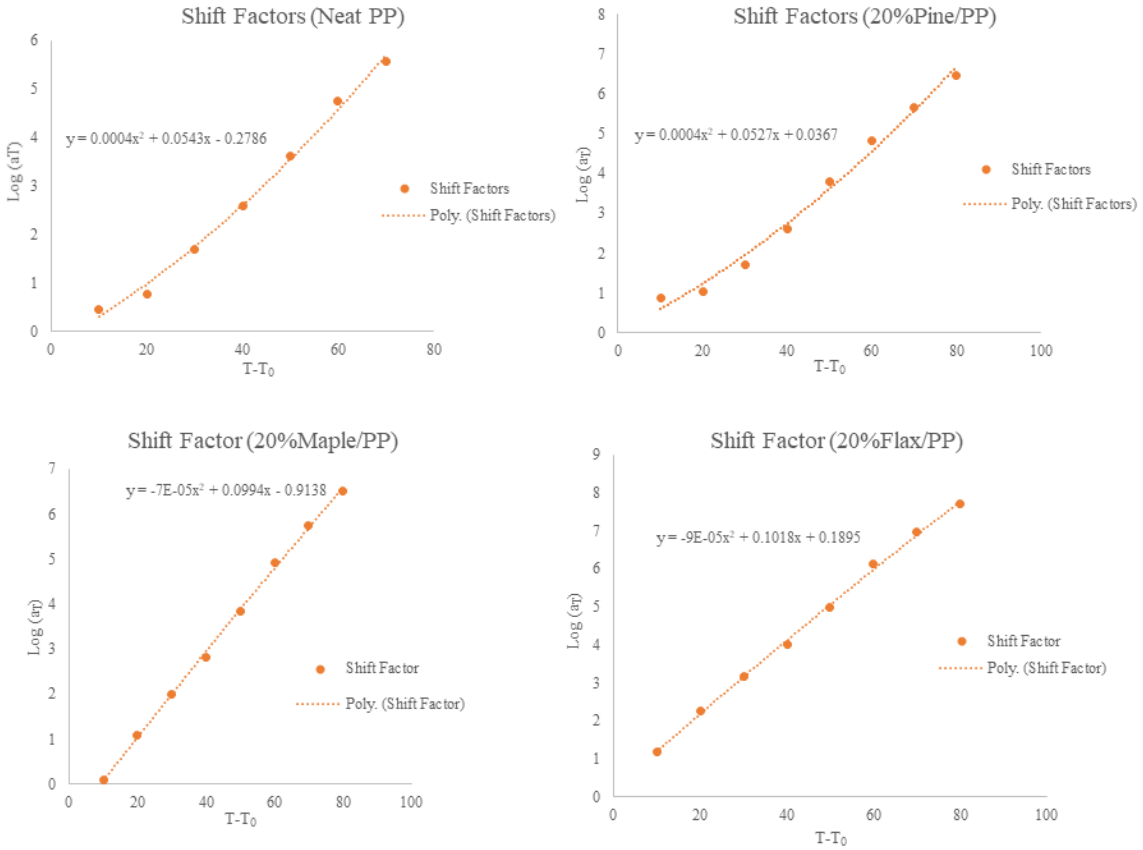

Figure 19. Williams-Landel-Ferry plots of horizontal shift factor

To generate a master compliance curve, creep compliance curves measured at different temperatures horizontally shifted in reference to a specific temperature. A master compliance curve provides information on the long-term behavior of a material at a reference temperature. The creep behavior curves of the Neat PP reinforced with different natural fibers at different temperatures are presented in Figure 21 to Figure 23.

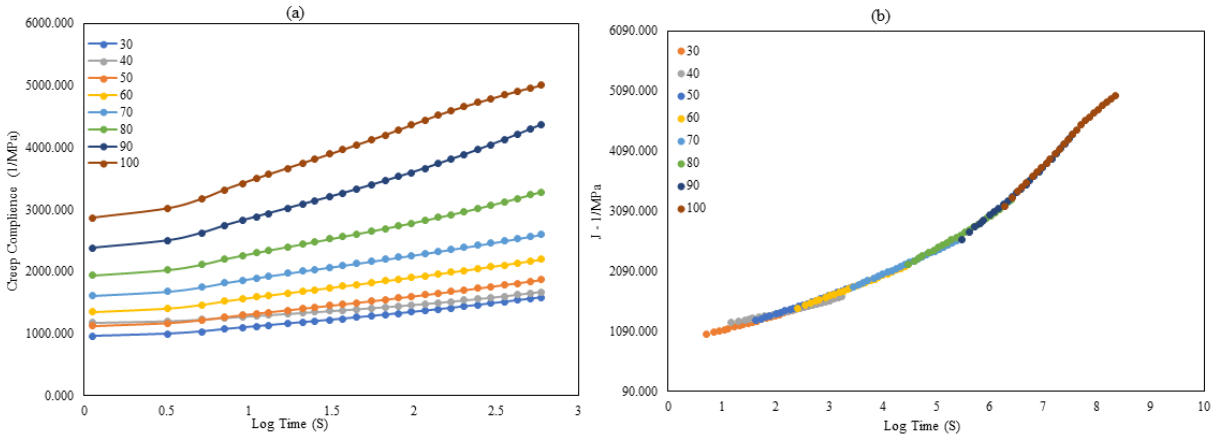

Figure 20. (a) Creep compliance curve at different temperatures for Neat PP (b) The master curve for creep compliance at 30 ºC for Neat PP

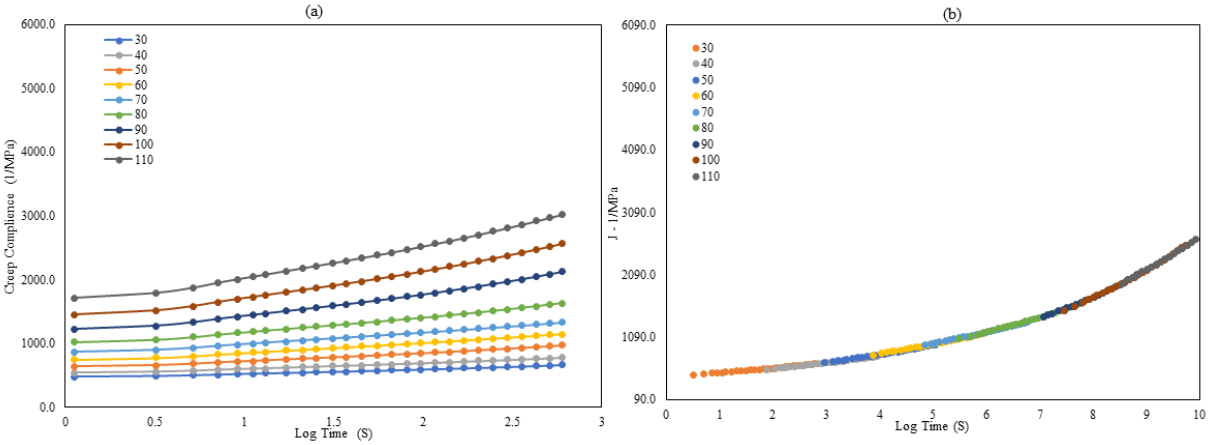

Figure 21. (a) Creep compliance curve at different temperatures for 20%Pine (b) The master curve for creep compliance at 30 ºC for 20%Pine

As seen in the graphs, creep curves for 30℃ and 40℃ are very similar and overlapping. However, it is 50℃, and above that temperature, the difference between the creep behaviors at different temperatures can be differentiated from each other. Also, with increasing temperature,

the creep compliance is increase which was anticipated. This is consistent with the other studies done on creep behavior of the natural fiber-reinforced composites [46,59].

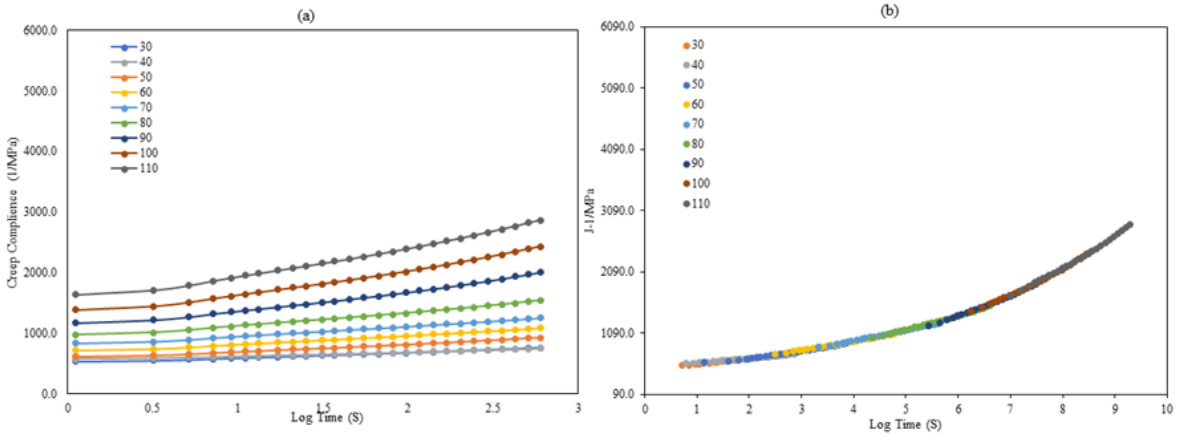

Figure 22. (a) Creep compliance curve at different temperatures for 20%Maple (b) The master curve for creep compliance at 30 ºC for 20%Maple

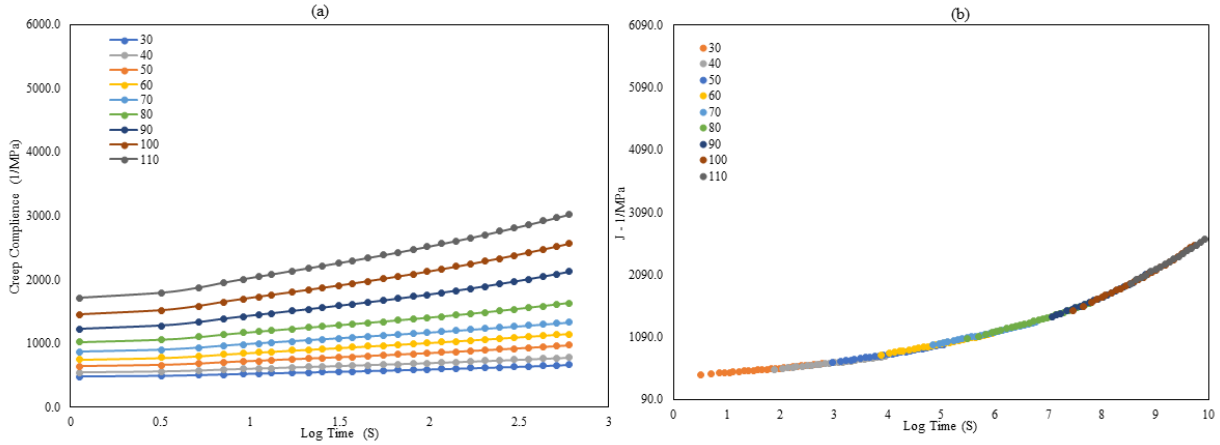

Figure 23. (a) Creep compliance curve at different temperatures for 20%Flax (b) The master curve for creep compliance at 30 ºC for 20%Flax

30°C temperature was selected as the reference temperature to shift to the right on the time axis to generate the master compliance curve. For calculating the shift factors, MATLAB® code was used, and the result of the shifted curve is shown in Figure 24. The resulting master curve provides the accelerated creep behavior up to 10^9 seconds which is 32 years if temperature up to 100°C was used [8]. Thus, to predict the creep behavior of the composites reinforced with flax, pine, or maple, only the creep test up to 100°C needs to be run for 10 minutes instead of 32 years.

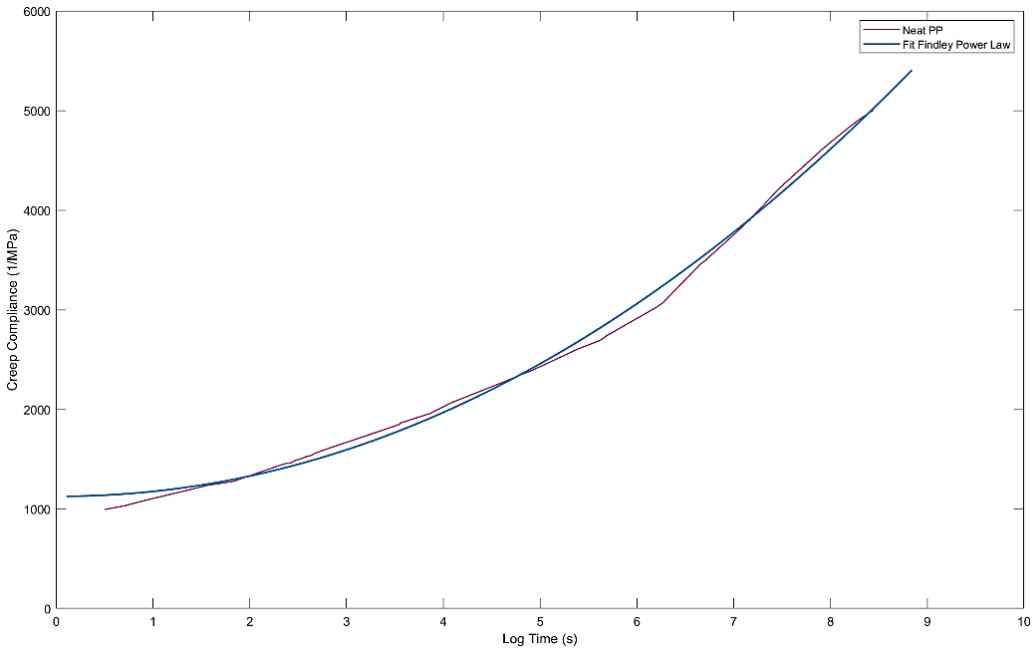

Figure 24. The master curve of creep compliance for Neat PP at 30 ºC and Findley Power Law fit

Figure 24 above shows the fitted curve of the neat PP using the Fit Findley Power Law. Again, a slight deviation was observed between the experimental data and power law; however, it seems to be an agreement between the experiment data and Fit Findley Power Law.

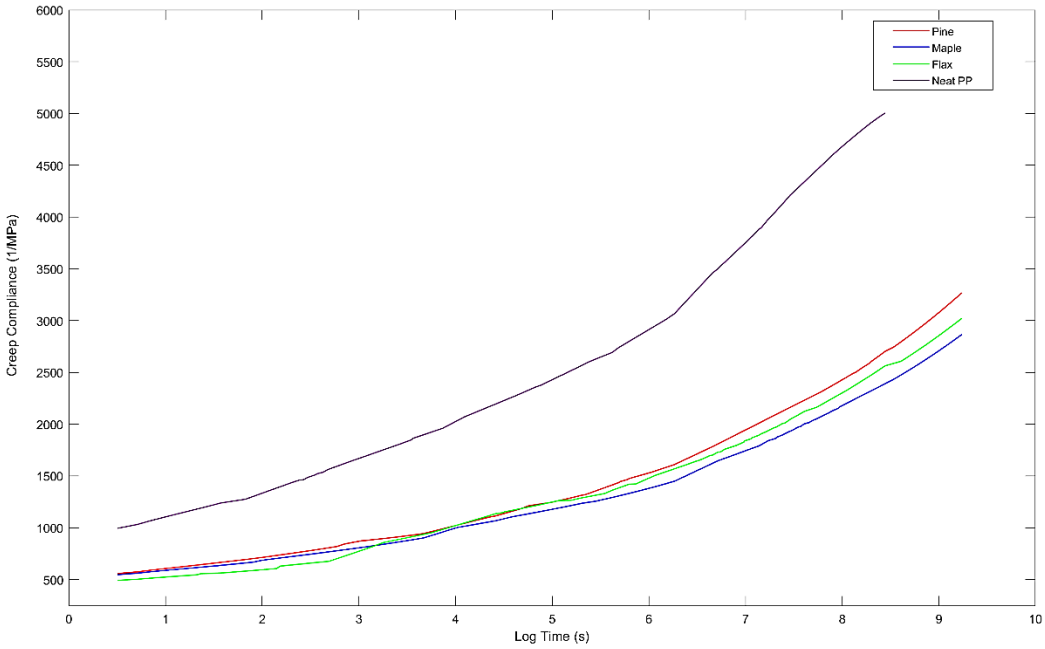

Figure 25. Creep compliance master curve for Neat PP and PP reinforced with natural fiber

Figure 25 shows creep compliance master curves by shifting the curves horizontally at 30℃ reference temperature. It was observed from the graph that Neat PP has a higher deformation compared to the PP reinforced with the natural fibers. PP having the higher deformation is due to the ductility of the materials and due to the constant loading polymer chain start to uncoil, thus leading to the deformation [71]. From Figure 25, adding the 20% natural fiber improved the resistance to creep behavior of the composites as adding the natural fibers increase the brittleness of the composites. In addition, a composite made with 20% flax fiber has lower creep initially until $10^{3.5}$ seconds, while 20% maple and pine have higher deformation than flax fiber. It is due to the maple and pine having a higher hemicellulose content than the flax fibers.

In addition, after $10^{3.5}$ seconds, the composite with 20% pine fiber shows less resistance to creep. It could be due to the higher content of the lignin present in the pine flour. On the other hand, maple has the lowest amount of cellulose compared to flax fibers; thus, it shows higher resistance to creep than the flax after $10^{3.5}$ seconds. Again creep phenomena of the fiber-reinforced are complex and depend on many factors such as polymer/fiber or interfacial particle strength, load transfer from matrix to fiber, and temperature [71].

For each generated master curve, coefficients for Findley Power Law Equation (4) and R-square of the fits are calculated and presented in Table 10 below. As mentioned before, A is the time-dependent coefficient, n is the stress-independent coefficient, and J_0 is the time-independent or elastic creep compliance. It can be seen from the table that with the addition of the 20% flax producing the n values to be 2.099. In comparison, the neat PP has the n value of 2.193. Therefore, it can be inferred that with the addition of the flax stress independent coefficient was reduced.

Table 10. Parameters in Findley Power Law equation

Composites	**J_0 (1/MPa)**	**A**	**n**	**R-Square**
Neat PP	1188.0 ± 33.0	35.81 ± 4.67	2.193 ± 0.061	0.9956
20% Pine	671.5 ± 11.4	14.30 ± 1.51	2.305 ± 0.049	0.9967
20% Flax	581.5 ± 25.6	21.76 ± 3.58	2.099 ± 0.074	0.9918
20% Maple	647.3 ± 15.7	11.68 ± 1.51	2.344 ± 0.059	0.9955

5.3. Thermal Analysis

To identify the thermal degradation and stability of the various samples, TGA analysis was performed. Figure 26 shows the mass loss over the various temperature for the neat PP and PP with additives and natural fibers and additives. Based on the figure, it could be seen that TGA curves show the one-step degradation for all samples. In addition, the TGA curve for the Neat PP and PP/additives indicates that thermal decomposition of the Neat PP was at temperature ranges of 250℃ to 325℃ when the natural zeolite (NZ) and white clay (WC) were added to the PP it shows much thermal stability of the samples. Therefore, it can be inferred from that graph that Neat PP has poor thermal stability, similar to the trend observed in the study done in the past [72]. For the PP with natural zeolite (PNZ), the thermal decomposition of the sample was at temperature ranges of 250℃ to 350℃, and PP with the white clay (PWC) was at 275℃ to 400℃.

On the contrary, adding the synthetic zeolite (SZ) and volcanic pozzolan do not affect the thermal stability of the PP samples. In addition, additives with pine and flax fiber-based composites improved the thermal stability. As seen in the graphs, pine and flax composite samples without the additives degraded at a much faster rate than with the additives. It was interesting to see that adding the additives to maple fiber composites did not significantly change the thermal stability of the maple-based composites.

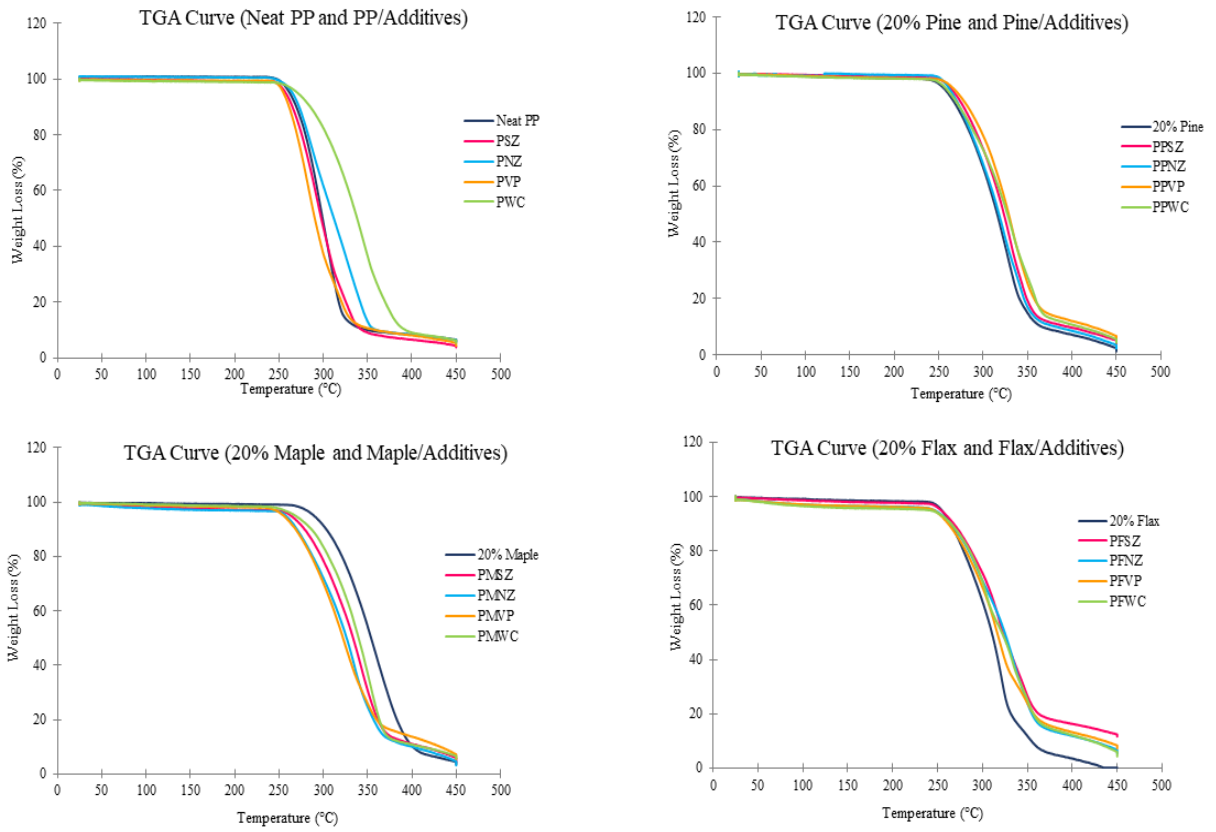

Figure 26. TGA curves

Figure 27 below represents the 1st derivative curve of the TGA analysis, representing the mass loss rate over the various temperature ranges from 25°C to 450°C. The first derivative graphs were plotted in the OriginPro® 2020 version of the software. First, the raw data and the temperatures were plotted in the software, then using the differentiate function under the analysis tab; it was plotted as temperature vs. derivative weight loss. Then, to clear the noise in the graph, the Adjacent-Averaging option was chosen under the smooth curve options. Finally, the point of the window was adjusted to get the smoother derivative curve of the data point collected for the composites. It is observed that the decomposition of the neat PP happens at 300°C. In contrast, when the white clay is added to the PP, the decomposition peak happens to around 355°C, and natural zeolite with PP is observed to be a two-step decomposition. In addition, composites

reinforced with pine fiber have a decomposition peak of around 325℃; however, adding the white clay seems to improve the thermal stability of the pine/PP composites.

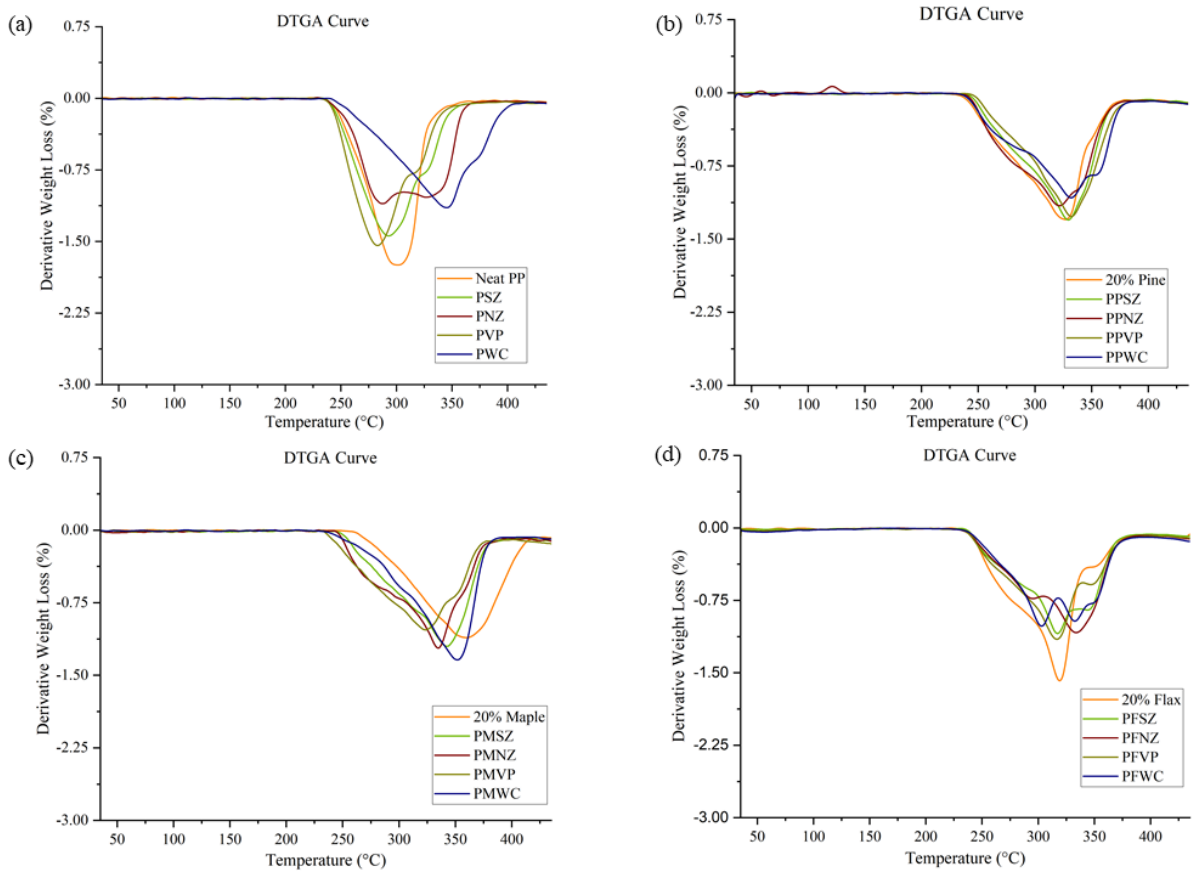

Figure 27. Derivative thermogravimetry (DTG) curve

Besides, composites reinforced with the flax fiber have a decomposition peak of around 325℃ but adding the natural zeolite and white clay, the decomposition peak happens at a much later temperature. In addition, flax/PP composites show the two-step degradation process; it could be the first degradation due to hemicellulose, and the second degradation was due to cellulose present in the flax fiber. The enhancement in the thermal stability of the composites with additives could be due to the presence of the quarts in the additives and the formation of the metal oxides in the PP and natural fiber surface [51]. It was observed that additives added to the composites reinforced with maple fibers did not significantly change the decomposition of the materials. It's due to maple fiber being coarse and while the inorganic fillers were in very fine powder. This

could have led to the inorganic porous fillers not being evenly dispersed in the matrix and forming the agglomeration with the maple fiber, as seen in the SEM image, Figure 33.

5.4. Fogging Test

The reflectometric (F) value of the tested glass plates was measured before and after putting in the thermostatic bath for 3hrs. The F value was calculated as per (6. Figure 28 shows the calculated F values of the composite, and it was recommended to have the F value greater than 85% [73]. It is seen from the graph that the Neat PP sample has a reflectometric value of 73.38 (±) 1.45%, which is far below the limit set by Hyundai and Ford. In contrast, PP with the porous fillers shows the higher reflectometric values and surpasses the limit set by Hyundai and Ford, especially the PP with white clay, which has an F value of 89.23 (±) 2.03%. White clay is the hydrated aluminum silicate that has a crystalline structure [37]. Due to the crystalline structure, it has a larger surface area that can absorb many times its weight [37]; therefore, PP with white clay is having higher F values as it adsorbs the larger amount of the volatile compounds from the neat PP compared to the synthetic zeolite, natural zeolite, and volcanic pozzolan [74].

When the maple fiber was added to the PP, the reflectometric value came out to be 85.11 (±) 3.27% on average, which is higher than the limit set by Ford and Hyundai. The reason for maple/PP having a higher F value than the neat PP is that the maple fiber improves the thermal decomposition of the composites, as seen in the DTGA curve of Figure 26. Furthermore, when the inorganic porous fillers were added to the maple/PP composites, it improved the reflectometric value. Out of all four inorganic fillers, natural zeolite increased the reflectometric value by almost 4.4%. Natural zeolite increases the F value because it has a larger surface area than synthetic zeolite and volcanic pozzolan; therefore, it can adsorb more radicals during the F test [49]. However, volcanic pozzolan gave the reflectometric value below the Hyundai limit, which is 85%. Volcanic

pozzolan gives a low F value is due to the structure of the volcanic pozzolan. Volcanic pozzolan does not absorb much of the volatile compound as zeolite and white clay as it does not have tightly packed crystalline structures [75]. Therefore, during the fogging test, some of the VOCs condensed on the glass plate and reduced the ability of the light to pass through.

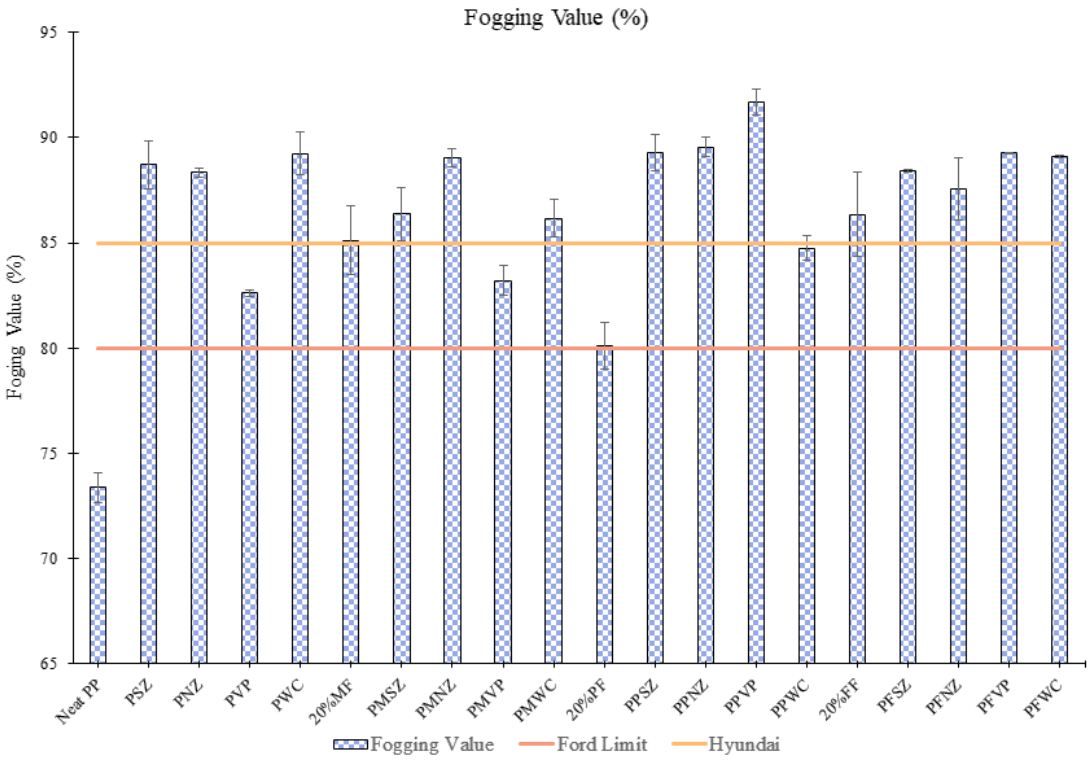

Figure 28. F method test value (%)

In contrast, when the pine fiber was added to the composites, it gave the F value on the average of 80.11 (±) 2.22%, which was below the limit set by Hyundai. In addition, even the TGA graph, Figure 26, for the pine/PP shows that pine/PP decomposed at a faster rate than the maple/PP. Similarly, inorganic porous fillers enhanced the F value of the pine/PP composites. Another reason for pine/PP having less F value is due to pine having a higher percentage of lignin which contributes to the hydrocarbon emission during the thermal degradation [76]. Furthermore, synthetic zeolite and natural zeolite increase the F value by almost 10%. Since these porous fillers have a smaller surface area, they can absorb twice their own weight [36,49]. Another reason is that

those fillers have an open porous complex crystallographic structure that can trap the VOCs and other gases during the thermal degradation, which prevents those gases getting condense on the surface of the glass [36,49].

In contrast, flax/PP had the F value on the average 86.35 (±) 4.03% higher than the maple and pine fiber composites. The reason for the flax/PP having the higher F value is due to the chemical constituents of the flax fiber. As shown in Table 5, flax fiber has a higher amount of cellulose than maple and pine fiber. As mentioned before, cellulose has high thermal stability, which can resist degradation for a long time under constant heat [15]. A similar pattern was observed with the flax/PP composites with the inorganic porous fillers. Increased in the F value of the flax/PP with the addition of the inorganic filler is due to the porous structures made up of the interconnected cavities, which can hold the various oxidation and thermal degradation gasses preventing from getting condensed on the surface of the glass [77].

The gravimetric (G) value of the tested aluminum foil was measured before and after putting it in the thermostatic bath for 16 hours. The G value was calculated as per Equation (7). Figure 29 shows the calculated G values of the composite, and it was recommended to have the G value less than 1 and 5mg [73]. It can be seen from the graph that neat PP has a G value of 1.05 (±) 0.07mg, which is higher than the literature limit of 1mg. It is due to PP was unable to resist the thermal degradation, as observed in the TGA graphs of the neat PP in Figure 27. which leads to chain breakage, and formed radicals start to emit. Whereas adding the natural zeolite reduced the average G value to 0.55 (±) 0.07mg. Furthermore, adding the white clay and volcanic pozzolan to the PP reduced the G value below the literature limits.

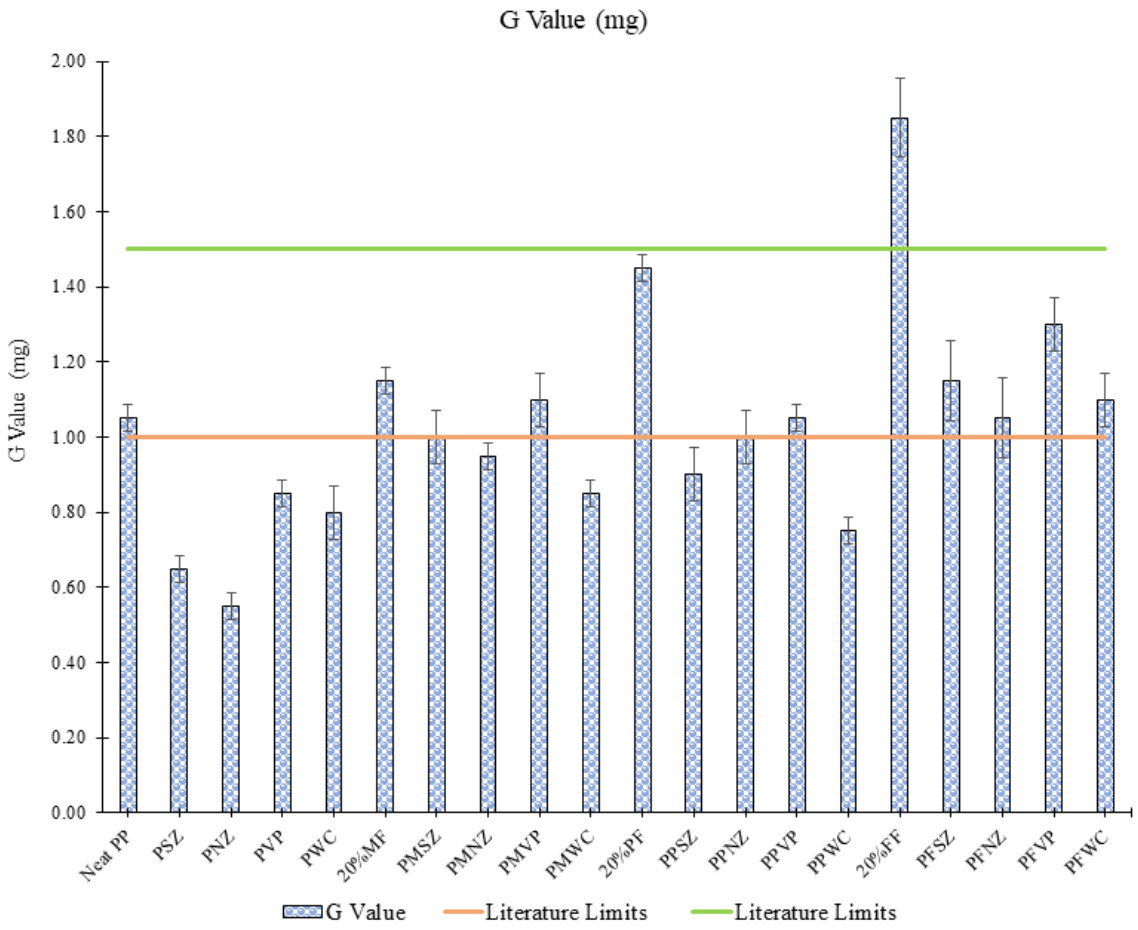

Figure 29. G method test value (mg)

On the contrary to the F test, adding the maple fiber to the PP increased the G value to 1.15 (±) 0.07mg on average. Therefore, an increase in the G value after adding to the PP is due to the maple fiber constituents. As maple fiber comprises cellulose, hemicellulose, and lignin, cellulose and hemicellulose contribute to the hydrocarbon emission during thermal degradation. This results in a higher amount of condensation on the foil. Since the G test was done under the 16 hours time compared to the F test, which was 3 hours; therefore, the emission from these constituents was higher in the G test. Even with the G test, adding the inorganic porous fillers decreased the G value. Adding the white clay to the maple/PP was more effective in reducing the G value as white clay had a higher surface area to hold twice its weight. Also, the G test was done for the 16 hours time

frame. Therefore, it could be inferred that white clay can endure the constant heat for a more extended period as it has a higher amount of silicate and other organic content.

Like the maple fiber, adding the pine fiber to the PP, G value increased to 1.45 (±) 0.07mg on average. As mentioned before, pine fiber has a higher amount of lignin than maple. Because of this, pine/PP gave a higher G value than the maple/PP. In addition, lignin has high thermal stability so that it would have resist thermal degradation under a temperature of 100℃. However, the G test was performed for the 16 hours under the 100℃, which could be one reason why lignin starts to decompose during the G test. Furthermore, during the thermal degradation, lignin releases the hydro carboxyl group, which was the main contributor to fogging emission [76]. Besides, adding the inorganic porous filler reduced the G value as expected. White clay was more effective than the zeolite and volcanic pozzolan in lowering the G value of the pine/PP composites. Again, the white clay has a higher surface area, which can trap more emitted organic compounds during thermal degradation [36,49].

Similar to the maple and pine fiber, flax/PP increased the G value to 1.85 (±) 0.21mg on average, which was higher than the literature limit of 1 and 1.5mg. However, the flax has a lower G value than maple and pine fiber because the fiber has a higher amount of cellulose constituents. During thermal degradation, cellulose forms volatiles such as methane, carbon monoxide, and carbon dioxide [76]. This results in a higher amount of the formation of condensation on the aluminum foil, which increased the mass of the foil. Furthermore, TGA graphs of the flax/PP in Figure 26 showed that flax/PP without the additives decompose faster after reaching 275℃, so it can be concluded that flax/PP is not thermal stable under the constant temperature for the more extended period. As expected, adding the porous fillers decrease the G value; however, it did not produce the G value below the 1mg limit. Adding the natural zeolite reduced the G value to 1.05

(±) 0.21mg. As mentioned before, zeolite has a very complex porous crystalline structure that can trap the oxidation and thermal gasses, preventing the condensation of the gases on the surface of the foil [36,49].

Table 11. % Drop in G and F values

	% Drop in G value	% Drop in F value
Synthetic Zeolite		
PP	38.10	17.28
Maple	13.04	1.47
Pine	37.93	10.26
Flax	37.84	2.35
Avg.	31.73	7.84
Natural Zeolite		
PP	47.62	16.94
Maple	17.39	4.40
Pine	31.03	10.54
Flax	43.24	1.39
Avg.	34.82	8.32
Pozzolan		
PP	19.05	11.19
Maple	4.35	-2.28
Pine	27.59	12.63
Flax	29.73	3.28
Avg.	20.18	6.21
White Clay		
PP	23.81	17.76
Maple	26.09	1.23
Pine	48.28	5.47
Flax	40.54	3.08
Avg.	34.68	6.89

Note: Values are in %.

The % drop in the G and F values due to the inorganic porous fillers was presented in Table 11. It can be observed that, on average, natural zeolite and synthetic zeolite were more effective in reducing the G and F values. Furthermore, zeolite is more effective in improving the G and F value than white clay and volcanic pozzolan. As mentioned before, zeolite is a type of hydrated

aluminosilicate mineral with a framework of tetrahedra consisting of four oxygen atoms surrounded by silicon [77]. This network has open cavities in the form of channels and cages, which traps oxidative and thermal gases, thus reducing the emission of the VOCs. It can be seen from Figure 30 that the compression molded plate has bubbly and rough surface which could impact the F and G test. Therefore, to better understand the F and G results, test needs to performed on the injected molded panels.

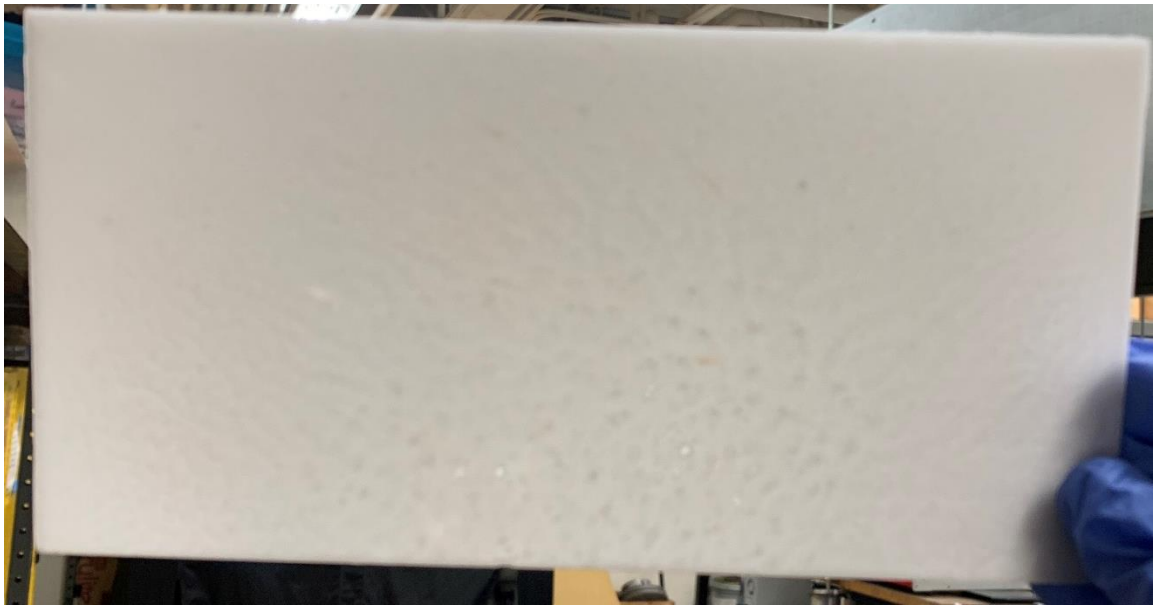

Figure 30. Surface of the compression molded plate

5.5. Image Analysis

Figure 31 shows the SEM images of the fractured surfaces of the tensile specimen of the Neat PP and composites reinforced with the natural fibers. SEM Images for Neat PP show the ductile fracture surface, whereas the composites show the brittle and fracture surface. It is inferred from the images that polymer chains are taking the loads in the Neat PP samples during the tensile test. However, when the natural fibers are added to the matrix, fibers are carrying the loads. Due to the excessive tensile stress, a crazing phenomenon is observed, leading to the micro-void formation and small fibrils, as seen in Figure 31(a) [78]. SEM images for the composites reinforced

with the natural fibers match the images in the literature [61,79]. In the composite, fibers were debonded and pulled out from the matrixes creating voids on the surface due to the poor interfacial adhesion and poor bonding of the polymer and fiber [61,79].

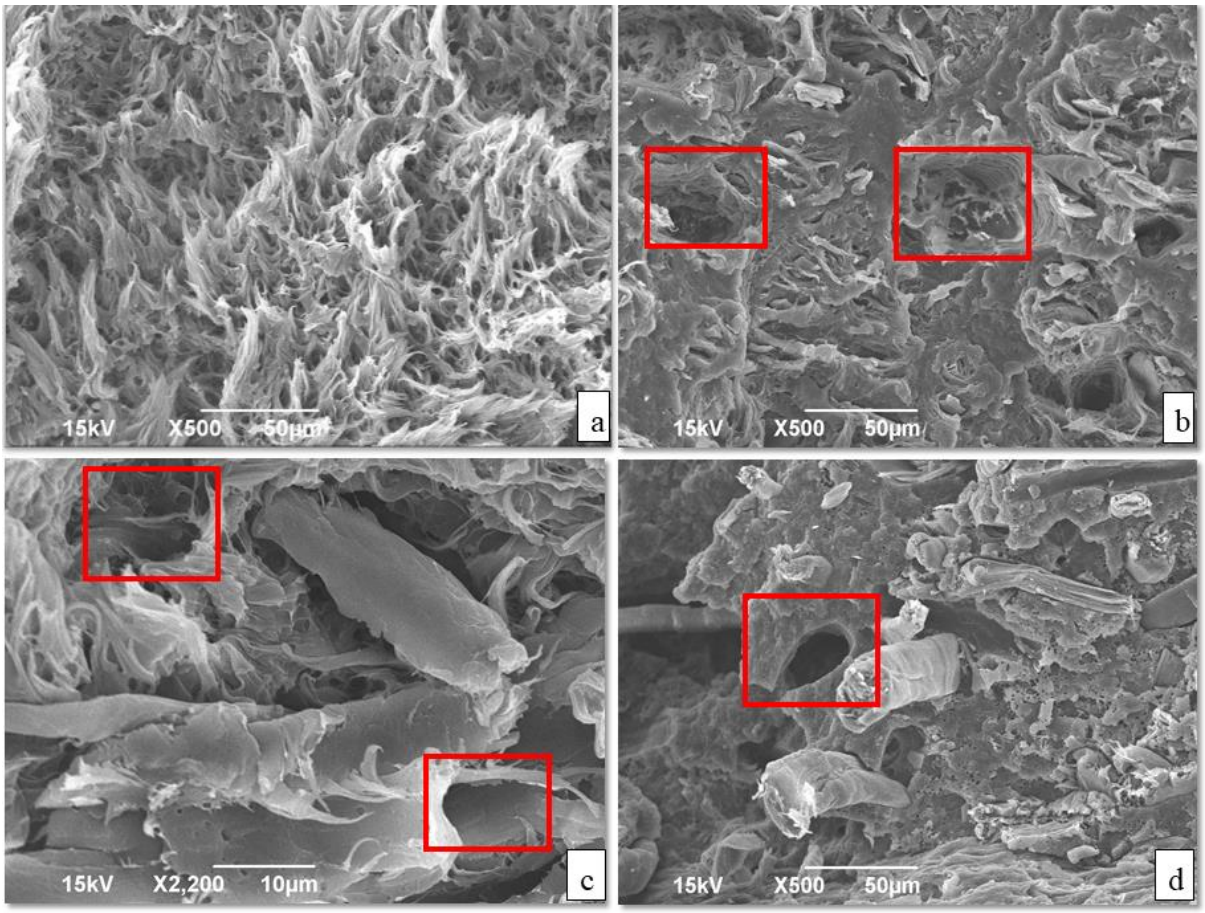

Figure 31. SEM Images (a) Neat PP, (b) Pine/PP, (c) Maple/PP and (d) Fax/PP

Note: Red square shows the fiber pull out and debonding of the fiber from the polymer matrix

Figure 32, Figure 33, and Figure 34 show the SEM images of the fractured tensile specimen reinforced with natural fibers and 3% additives. It is observed from the images that additives such as white clay (WC), volcanic pozzolan (VP), and synthetic zeolite (SZ) are well dispersed into the biocomposites. Furthermore, Figure 32 and Figure 33 show that pine and maple flour have a lower aspect ratio and smaller particle size than the flax fibers, which explains the composites reinforced

with pine and maple having lower tensile properties than the flax fiber. In addition, fiber separation from the polymer matrix is observed from the morphology analysis of the biocomposite surfaces.

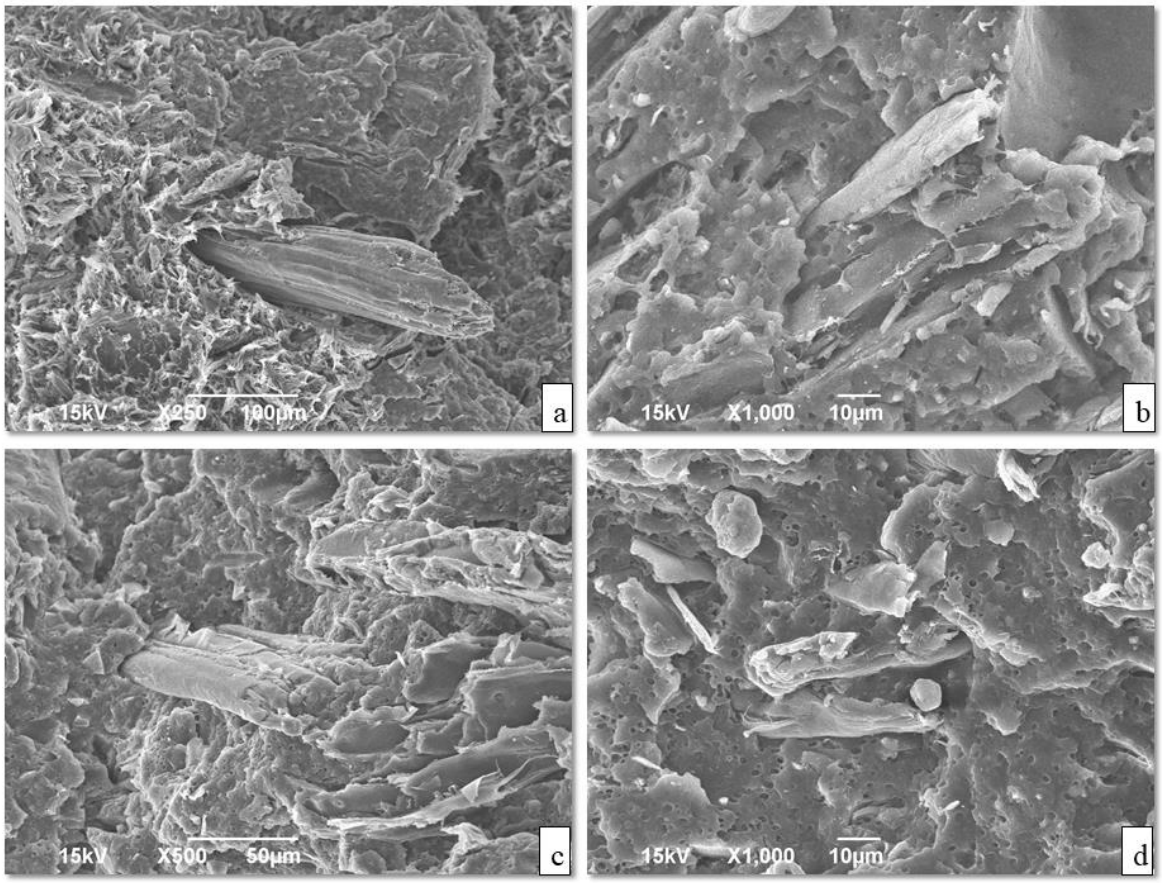

Figure 32. SEM Images (a) Pine/PP, (b) Pine/PP/WC, (c) Pine/PP/VP, and (d) Pine/PP/SZ

Figure 34 below shows the biocomposites reinforced with flax fibers and 3% additives. It is noticeable from the images that flax fibers have a high aspect ratio (length to diameter); thus, it has less pull-out effect compared to the maple and pine fibers. Also, the flax fiber having a higher aspect ratio produces the higher tensile strength result, which is confirmed by the morphology images taken in SEM. It's seen from those SEM images that there is low compatibility between the fiber, pozzolan, and the PP matrix since the fiber and pozzolan are hydrophilic and the PP matrix is hydrophobic in nature. Since the natural fiber and pozzolan attract the water and the moisture absorption is high, it leads to the weak interfacial adhesion and void spaces between fiber,

pozzolan, and PP, resulting in the debonding of the fiber from the PP. To overcome this issue, many researchers have used fiber modification, silane treatment, and using the coupling agents to reduce the moisture absorption by the fibers [15].

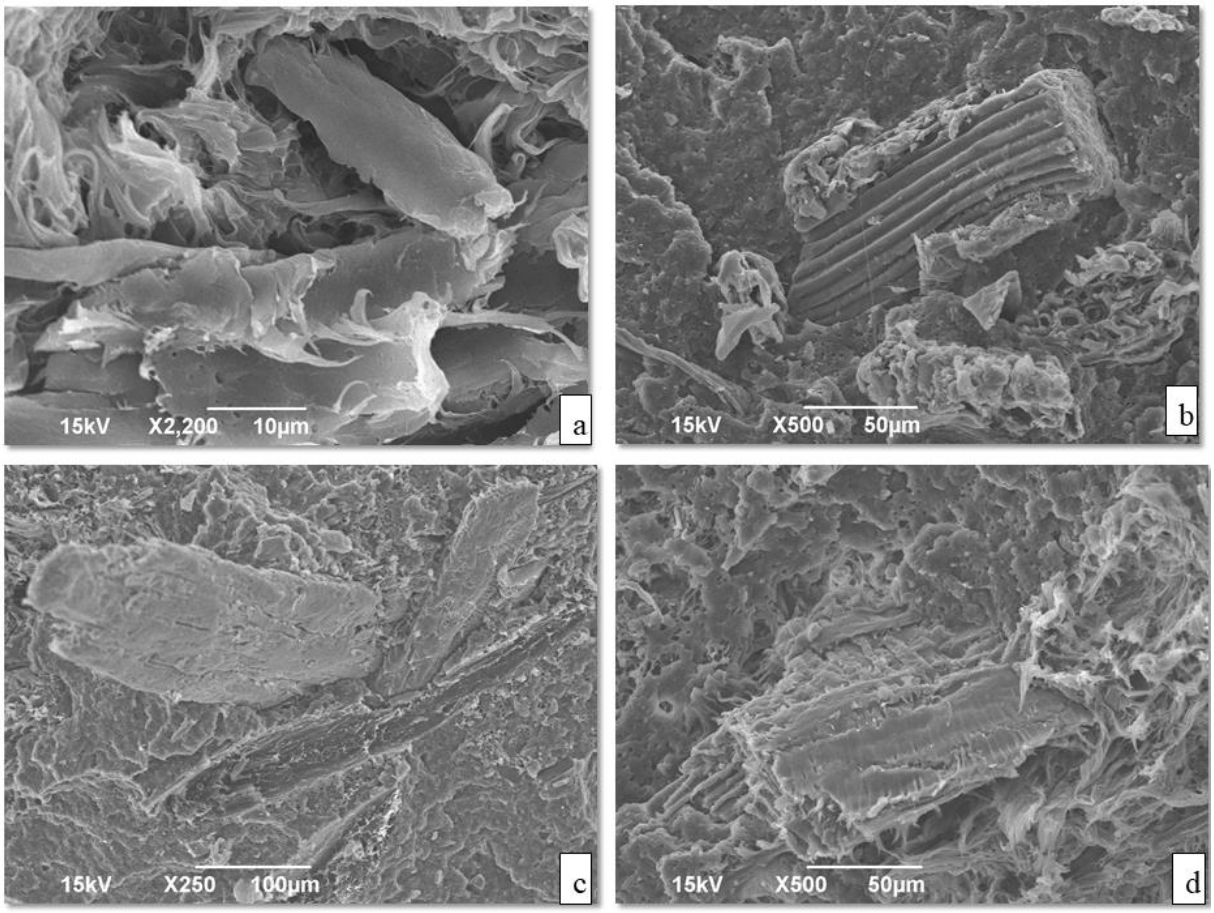

Figure 33. SEM Images (a) Maple/PP, (b) Maple/PP/WC, (c) Maple/PP/VP, and (d) Maple/PP/SZ

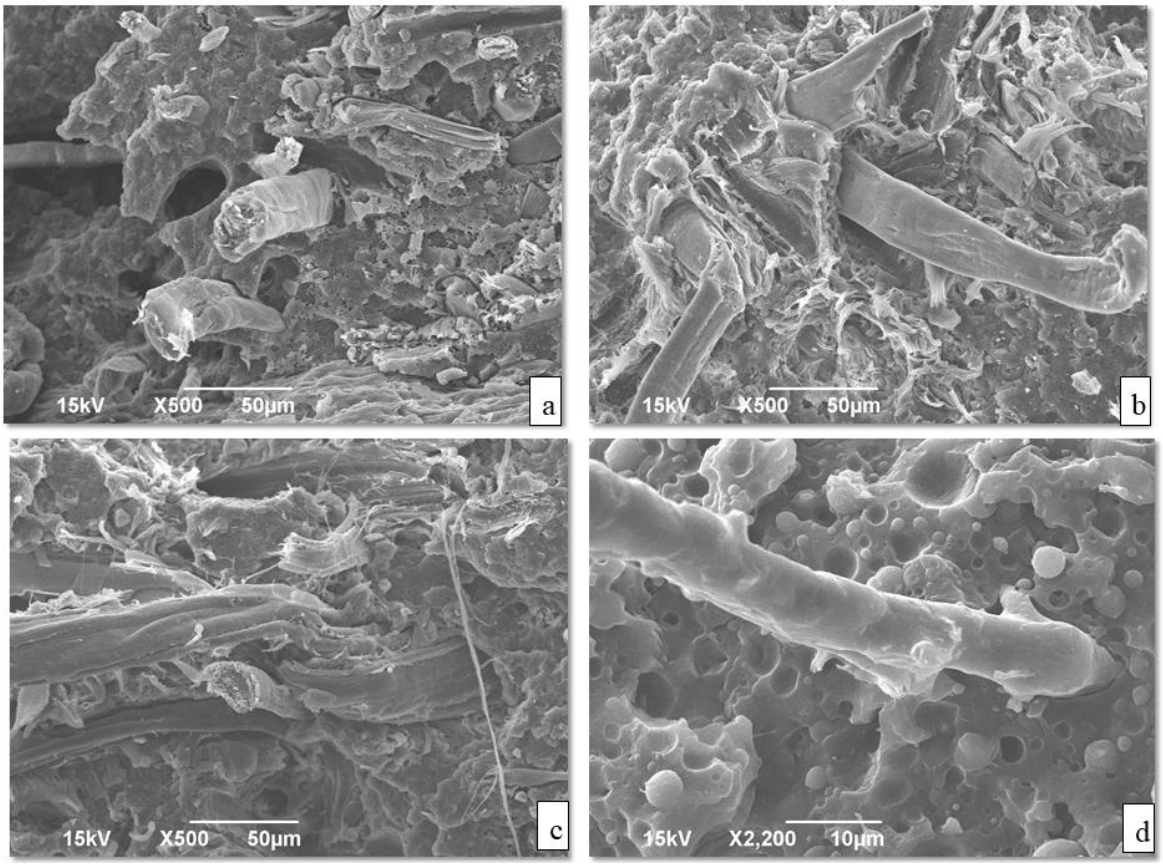

Figure 34. SEM Images (a) Flax/PP, (b) Flax/PP/WC, (c) Flax/PP/VP, and (d) Flax/PP/SZ

5.6. Statistical Analysis

ANOVA one-way variance statistical analysis was performed on the mechanical properties. Table 12 shows the variance results at $\alpha = 0.05$ due to adding the additives such as synthetic zeolite, natural zeolite, volcanic pozzolan, and white clays to biocomposites. The black shaded square represents that the data is statistically significant ($p<0.05$), and the unshaded circle represents that data is statistically insignificant ($p>0.05$). The flexural strength reported for pine with all four additives is statistically insignificant, and maple with all four additives is statically insignificant for the flexural properties such as strength and modulus.

ANOVA one-way variance statistical analysis was also performed for the F and G test method. Maple and flax with the additives show that means data is statistically insignificant for

the F test to reject the null hypothesis. In addition, the F value for the PP and pine with additives is statistically significant compared to the maple and flax with the additives. Besides, the G values for the flax with the additives are significant compared to the pp, maple, and pine with the additives.

Table 12. Result of the ANOVA statistical analysis

Properties	PP/ additives	Pine/ additives	Maple/ additives	Flax/ additives
Tensile strength (MPa)	■	■	■	■
Tensile modulus (GPa)	■	■	■	■
Flexural strength (MPa)	■	○	○	■
Flexural modulus (GPa)	■	■	○	■
Impact Strength (kJ/m^2)	■	■	■	■
F Test Method (%)	■	■	○	○
G Test Method (mg)	○	○	○	■

6. CONCLUSION AND FUTURE RECOMMENDATIONS

Due to the environmental and regulatory pushing the automobile industry to incorporate more bio-based materials, natural fibers find their way to be utilized in automobile applications. However, natural fiber has its challenges, such as thermal degradation, VOC emission during the degradation, and durability issues. Porous filler was added to the biocomposites to target the responsible constituents to minimize the VOCs emission during the thermal degradation. The creep behavior and the thermal analysis were carried out on the samples without the additives to over the durability issue.

Also, the mechanical properties such as tensile properties, flexural properties, and impact strength were investigated to see whether adding the porous filers affects the strength and modules of the biocomposites. Based on the mechanical tests, it was concluded that adding the 3% porous fillers did not hinder the tensile and flexural properties of the biocomposites. On the contrary, it enhanced the impact strength of the biocomposites. To further analyze the impact strength results, the area near the fractured surface by making the cut perpendicular to the fractured surface needs to be analyzed under the SEM to confirm the crazing sites.

Also, the long-term behavior of the composites was modeled using the TTS principle. It was inferred that adding natural fibers such as maple and flax fiber has a higher resistance to creep than the composites with pine and neat PP. It can be due to the chemical constituents present in the pine flour and particle size differences. In addition, TGA analysis indicates that the thermal stability of the PP, pine, and flax fiber-based composites improved with the porous filler. In contrast, the thermal stability of the composites reinforced with the maple did not improve with the addition of the porous filler. The reflectometric (F) test and gravimetric (G) test methods are used as per ISO 6452 to analyze the reduction of fogging behavior. It can be inferred that adding

the porous filler enhanced the reflectometric value. The F values for the biocomposites made with porous filler surpass the limit set by Hyundai and Ford. In addition, further study needs to be performed on the injected molded panels. As it was seen that the compression-molded plate had bubbles on the surface, which might have allowed the VOCs to pass through during the test. With the injection-molded panels, the surface will be smooth without the bubbles, which further helps trap the gasses inside and improve the fogging behavior.

From the SEM images, poor interfacial adhesion and bonding of the polymer and fiber were observed. Therefore, one of the future recommendations is to improve interfacial adhesion and bonding of the polymer and fiber through surface modification, such as physical or biological modification [80,81]. Another way to improve interfacial adhesion and bonding of the polymer and fiber is by adding the coupling agents such as Maleic anhydride grafted polypropylene (MA-PP) and maleic anhydride grafted ethylene-propylene-diene copolymer (MA-EPDM) [62].

Another challenge with the natural fiber composites is fire degradation, limiting the application of the composites [63]. However, fire retardants such as expandable graphite (EG), ammonium polyphosphate (APP), or metallic hydroxide, including magnesium hydroxide, can be used as additives to improve the fire degradation of the natural fiber composites [15,82]. Another method mentioned improving the fire-resistant capacity of the natural fiber composites includes impregnating the natural fiber with fire retardants before the processing, introducing the nanoparticles, or insulating composites with the intumescent coatings or fire barriers [83].

REFERENCES

[1] 2017, “Fiber Reinforced Polymer (FRP) Composites Market Analysis By Fiber Type (Glass, Carbon, Basalt, Aramid), By Application (Automotive, Construction, Electronic, Defense), By Region, And Segment Forecasts, 2018 - 2025,” Mark. Anal. Rep., p. 95.

[2] Reingruber, E., Reussner, J., Sauer, C., Standler, A., and Buchberger, W., 2011, “Studies on the Emission Behavior of Polypropylene by Gas Chromatography/Mass Spectrometry with Static Headspace or Thermodesorption,” J. Chromatogr. A, **1218**(21), pp. 3326–3331.

[3] Chen, J. Y., Müller, D. H., König, C., Nießen, K., and Müssig, J., 2010, “Spunlaced Flax/Polypropylene Nonwoven as Auto Interior Material: Acoustical and Fogging Performance,” J. Biobased Mater. Bioenergy, **4**(4), pp. 330–337.

[4] Birat, K. C., Panthapulakkal, S., Kronka, A., Agnelli, J. A. M., Tjong, J., and Sain, M., 2015, “Hybrid Biocomposites with Enhanced Thermal and Mechanical Properties for Structural Applications,” J. Appl. Polym. Sci., **132**(34), pp. 1–8.

[5] N E Naveen, P., and Yasaswi, M., 2013, “Experimental Analysis of Coir-Fiber Reinforced Polymer Composite Materials,” Int. J. Mech. Eng. Rob. Res, **2**(1), pp. 10–18.

[6] Taylor, C., Amiri, A., Paramarta, A., Ulven, C., and Webster, D., 2017, “Development and Weatherability of Bio-Based Composites of Structural Quality Using Flax Fiber and Epoxidized Sucrose Soyate,” Mater. Des., **113**, pp. 17–26.

[7] Christian, S. J., 2019, “Natural Fibre-Reinforced Noncementitious Composites (Biocomposites),” *Nonconventional and Vernacular Construction Materials: Characterisation, Properties and Applications*, pp. 169–187.

[8] Amiri, A., Hosseini, N., and Ulven, C. A., 2015, “Long-Term Creep Behavior of Flax/Vinyl Ester Composites Using Time-Temperature Superposition Principle,” J. Renew. Mater., **3**(3), pp. 224–233.

[9] Radkar, S. S., Amiri, A., and Ulven, C. A., 2019, “Tensile Behavior and Diffusion of Moisture through Flax Fibers by Desorption Method,” Sustain., **11**(13), pp. 1–10.

[10] Chandramohan, D., and Marimuthu, K., 2011, “A Review on Natural Fibers,” Int. J. Res. Rev. Appl. Sci., **8**(2), pp. 194–206.

[11] Koohestani, B., Darban, A. K., Mokhtari, P., Yilmaz, E., and Darezereshki, E., 2019, “Comparison of Different Natural Fiber Treatments: A Literature Review,” Int. J. Environ. Sci. Technol., **16**(1), pp. 629–642.

[12] Tajvidi, M., Falk, R. H., and Hermanson, J. C., 2006, “Effect of Natural Fibers on Thermal and Mechanical Properties of Natural Fiber Polypropylene Composites Studied by Dynamic Mechanical Analysis,” J. Appl. Polym. Sci., **101**(6), pp. 4341–4349.

[13] Amiri, A., Ulven, C. A., and Huo, S., 2015, "Effect of Chemical Treatment of Flax Fiber and Resin Manipulation on Service Life of Their Composites Using Time-Temperature Superposition," Polymers (Basel)., **7**(10), pp. 1965–1978.

[14] AlMaadeed, M. A., Kahraman, R., Noorunnisa Khanam, P., and Madi, N., 2012, "Date Palm Wood Flour/Glass Fibre Reinforced Hybrid Composites of Recycled Polypropylene: Mechanical and Thermal Properties," Mater. Des., **42**, pp. 289–294.

[15] Azwa, Z. N., Yousif, B. F., Manalo, A. C., and Karunasena, W., 2013, "A Review on the Degradability of Polymeric Composites Based on Natural Fibres," Mater. Des., **47**, pp. 424–442.

[16] John, M. J., and Thomas, S., 2008, "Biofibres and Biocomposites," Carbohydr. Polym., **71**(3), pp. 343–364.

[17] Onuaguluchi, O., and Banthia, N., 2016, "Plant-Based Natural Fibre Reinforced Cement Composites: A Review," Cem. Concr. Compos., **68**, pp. 96–108.

[18] Elmogahzy, Y. E., 2020, "Engineering Textiles," *Integrating the Design and Manufacture of Textile Products*, Elsevier, pp. 191–222.

[19] Fuqua, M. A., Huo, S., and Ulven, C. A., 2012, "Natural Fiber Reinforced Composites," Polym. Rev., **52**(3), pp. 259–320.

[20] Pickering, K. L., Efendy, M. G. A., and Le, T. M., 2016, "A Review of Recent Developments in Natural Fibre Composites and Their Mechanical Performance," Compos. Part A Appl. Sci. Manuf., **83**, pp. 98–112.

[21] Kumar, R., Ul Haq, M. I., Raina, A., and Anand, A., 2019, "Industrial Applications of Natural Fibre-Reinforced Polymer Composites–Challenges and Opportunities," Int. J. Sustain. Eng., **12**(3), pp. 212–220.

[22] Yan, L., Chouw, N., and Jayaraman, K., 2014, "Flax Fibre and Its Composites - A Review," Compos. Part B Eng., **56**, pp. 296–317.

[23] Garkhail, S. K., Heijenrath, R. W. H., and Peijs, T., 2000, "Mechanical Properties of Natural-Fibre-Mat -Reinforced Thermoplastics Based on Flax Fibres and Polypropylene," Appl. Compos. Mater., **7**(5–6), pp. 351–372.

[24] van den Oever, M. J. A., Bos, H. L., and van Kemenade, M. J. J. M., 2000, "Influence of the Physical Structure of Flax Fibres on the Mechanical Properties of Flax Fibre Reinforced Polypropylene Composites," Appl. Compos. Mater., **7**(5–6), pp. 387–402.

[25] Singleton, A. C. N., Baillie, C. A., Beaumont, P. W. R., and Peijs, T., 2003, "On the Mechanical Properties, Deformation and Fracture of a Natural Fibre/Recycled Polymer Composite," Compos. Part B Eng., **34**(6), pp. 519–526.

[26] Bodros, E., Pillin, I., Montrelay, N., and Baley, C., 2007, “Could Biopolymers Reinforced by Randomly Scattered Flax Fibre Be Used in Structural Applications?,” Compos. Sci. Technol., **67**(3–4), pp. 462–470.

[27] Adhikary, K. B., 2008, “Development of Wood Flour- Recycled Polymer Composite Panels As Building Materials.”

[28] Li, T., and Yan, N., 2007, “Mechanical Properties of Wood Flour/HDPE/Ionomer Composites,” Compos. Part A Appl. Sci. Manuf., **38**(1), pp. 1–12.

[29] Yeh, S. K., and Gupta, R. K., 2008, “Improved Wood-Plastic Composites through Better Processing,” Compos. Part A Appl. Sci. Manuf., **39**(11), pp. 1694–1699.

[30] Kim, J.-W., Harper, D. P., and Taylor, A. M., 2010, “Effect of Wood Species on the Mechanical and Thermal Properties of Wood–Plastic Composites,” J. Appl. Polym. Sci., **116**(5), pp. 2658–2667.

[31] Teymoorzadeh, H., and Rodrigue, D., 2015, “Biocomposites of Wood Flour and Polylactic Acid: Processing and Properties,” J. Biobased Mater. Bioenergy, **9**(2), pp. 252–257.

[32] Murayama, K., Ueno, T., Kobori, H., Kojima, Y., Suzuki, S., Aoki, K., Ito, H., Ogoe, S., and Okamoto, M., 2019, “Mechanical Properties of Wood/Plastic Composites Formed Using Wood Flour Produced by Wet Ball-Milling under Various Milling Times and Drying Methods,” J. Wood Sci., **65**(1).

[33] Stark, N. M., and Rowlands, R. E., 2003, “Effects of Wood Fiber Characteristics on Mechanical Properties of Wood/Polypropylene Composites,” Wood Fiber Sci., **35**(2), pp. 167–174.

[34] Qiang, T., Yu, D., Wang, Y., and Gao, H., 2013, “Polylactide-Based Wood Plastic Composites Modified with Linear Low Density Polyethylene,” Polym. - Plast. Technol. Eng., **52**(2), pp. 149–156.

[35] Howick, C. J., and Mccarthy, S. A., 1996, “Studies of Possible Chemical Emissions from PVC Articles Used in Indoor Applications and the Effect on Indoor Air Quality,” J. Vinyl Addit. Technol., **2**(2), pp. 134–142.

[36] Kim, H. S., Kim, S., Kim, H. J., and Kim, H. G., 2006, “Physico-Mechanical Properties, Odor and VOC Emission of Bio-Flour-Filled Poly(Propylene) Bio-Composites with Different Volcanic Pozzolan Contents,” Macromol. Mater. Eng., **291**(10), pp. 1255–1264.

[37] Kim, H. S., Lee, B. H., Kim, H. J., and Yang, H. S., 2011, “Mechanical-Thermal Properties and VOC Emissions of Natural-Flour-Filled Biodegradable Polymer Hybrid Bio-Composites,” J. Polym. Environ., **19**(3), pp. 628–636.

[38] Yousif, E., and Haddad, R., 2013, “Photodegradation and Photostabilization of Polymers, Especially Polystyrene: Review,” Springerplus, **2**(1), pp. 1–32.

[39] Strong, A. B., 2006, “Plastics: Materials and Processing,” Sci. Technol. Adv. Mater., **14**, p. 917.

[40] Arshad, A., 2015, “Analysis and Control of Emissions Arising from Stabilised Polypropylene and the Incorporated Additives,” Manchester Metropolitan University.

[41] Kostecki, P., Morrison, R., and Dragun, J., 2004, “Hydrocarbons,” *Encyclopedia of Soils in the Environment*, Elsevier Inc., pp. 217–226.

[42] Rabinowitz, H., and Vogel, S. B. T.-T. M. of S. S., eds., 2009, “Chapter 10 - Style and Usage for Organic Chemistry,” Academic Press, San Diego, pp. 399–425.

[43] Curran, K., and Strlič, M., 2015, “Polymers and Volatiles: Using VOC Analysis for the Conservation of Plastic and Rubber Objects,” Stud. Conserv., **60**(1), pp. 1–14.

[44] Bhat, G. S., 1997, “Plastics: Materials and Processing by A. Brent Strong,” *Materials and Manufacturing Processes*, Taylor & Francis Group, pp. 560–562.

[45] Tajvidi, M., and Simon, L. C., 2015, “High-Temperature Creep Behavior of Wheat Straw Isotactic/Impact-Modified Polypropylene Composites,” J. Thermoplast. Compos. Mater., **28**(10), pp. 1406–1422.

[46] Tajvidi, M., Falk, R. H., and Hermanson, J. C., 2005, “Time-Temperature Superposition Principle Applied to a Kenaf-Fiber/High- Density Polyethylene Composite,” J. Appl. Polym. Sci., **97**(5), pp. 1995–2004.

[47] Findley, W. N., Lai, J. S., Onaran, K., and Christensen, R. M., 1977, “Creep and Relaxation of Nonlinear Viscoelastic Materials with an Introduction to Linear Viscoelasticity.”

[48] Bennett, E. A., 2012, “Influence of Creep on the Stability of Pultruded Columns at Elevated Service Temperatures.”

[49] Kim, H.-S., and Kim, H.-J., 2010, “Influence of the Zeolite Type on the Mechanical–Thermal Properties and Volatile Organic Compound Emissions of Natural-Flour-Filled Polypropylene Hybrid Composites,” J. Appl. Polym. Sci., **116**(5), pp. 2658–2667.

[50] Kim, S. J., and Kim, H. A., 2019, “Characteristics of Eco-Friendly Kenaf Fiber-Imbedded Nonwoven for Automotive Application,” IntechOpen, **15**(1), p. 26.

[51] Kim, H. S., and Kim, H. J., 2008, “Influence of the Zeolite Type on the Mechanical-Thermal Properties and Volatile Organic Compound Emissions of Natural-Flour-Filled Polypropylene Hybrid Composites,” J. Appl. Polym. Sci., **110**(5), pp. 3247–3255.

[52] Kim, S., 2009, “The Reduction of Indoor Air Pollutant from Wood-Based Composite by Adding Pozzolan for Building Materials,” Constr. Build. Mater., **23**(6), pp. 2319–2323.

[53] Duvarcı, Ö. Ç., Akdeniz, Y., Özmıhçı, F., Ülkü, S., Balköse, D., and Çiftçioğlu, M., 2007, "Thermal Behaviour of a Zeolitic Tuff," Ceram. Int., **33**(5), pp. 795–801.

[54] Siregar, J. P., Salit, M. S., Ab Rahman, M. Z., and Mohd Dahlan, K. Z. H., 2011, "Thermogravimetric Analysis (TGA) and Differential Scanning Calometric (DSC) Analysis of Pineapple Leaf Fibre (PALF) Reinforced High Impact Polystyrene (HIPS) Composites," Pertanika J. Sci. Technol., **19**(1), pp. 161–170.

[55] Kaymakci, A., Gulec, T., Hosseinihashemi, S. K., and Ayrilmis, N., 2017, "Physical, Mechanical and Thermal Properties of Wood/ Zeolite/Plastic Hybrid Composites," Maderas Cienc. y Tecnol., **19**(3), pp. 339–348.

[56] Mengeloglu, F., and Karakus, K., 2008, "Thermal Degradation, Mechanical Properties and Morphology of Wheat Straw Flour Filled Recycled Thermoplastic Composites," Sensors, **8**(1), pp. 500–519.

[57] Hosseinihashemi, S. K., Eshghi, A., Ayrilmis, N., and Khademieslam, H., 2016, "Thermal Analysis and Morphological Characterization of Thermoplastic Composites Filled with Almond Shell Flour/Montmorillonite," BioResources, **11**(3), pp. 6768–6779.

[58] Tajvidi, M., and Takemura, A., 2010, "Thermal Degradation of Natural Fiber-Reinforced Polypropylene Composites," J. Thermoplast. Compos. Mater., **23**(3), pp. 281–298.

[59] Xu, Y., Wu, Q., Lei, Y., and Yao, F., 2010, "Creep Behavior of Bagasse Fiber Reinforced Polymer Composites," Bioresour. Technol., **101**(9), pp. 3280–3286.

[60] Amiri, A., Yu, A., Webster, D., and Ulven, C., 2016, "Bio-Based Resin Reinforced with Flax Fiber as Thermorheologically Complex Materials," Polymers (Basel)., **8**(4), pp. 1–14.

[61] Pérez, E., Famá, L., Pardo, S. G., Abad, M. J., and Bernal, C., 2012, "Tensile and Fracture Behaviour of PP/Wood Flour Composites," Compos. Part B Eng., **43**(7), pp. 2795–2800.

[62] Chui-gen, G., Yong-ming, S., Qing-wen, W., and Chang-sheng, S., 2006, "Dynamic-Mechanical Analysis and SEM Morphology of Wood Flour/Polypropylene Composites," J. For. Res., **17**(4), pp. 315–318.

[63] Kumar, R., Ul Haq, M. I., Raina, A., and Anand, A., 2019, "Industrial Applications of Natural Fibre-Reinforced Polymer Composites–Challenges and Opportunities," Int. J. Sustain. Eng., **12**(3), pp. 212–220.

[64] Yan, L., Chouw, N., and Jayaraman, K., 2014, "Flax Fibre and Its Composites - A Review," Compos. Part B Eng., **56**, pp. 296–317.

[65] ASTM International, "ASTM D638-10 : Standard Test Method for Tensile Properties of Plastics."

[66] ASTM International, 2018, *ASTM D256-18 Standard Test Methods for Determining the Izod Pendulum Impact Resistance of Plastics*, West Conshohocken, PA.

[67] ASTM International, 2015, *ASTM D5418 - 15 Standard Test Method for Plastics: Dynamic Mechanical Properties: In Flexure (Three-Point Bending)*, West Conshohocken, PA.

[68] ASTM International, 2015, *ASTM D5023-15 Standard Test Method for Plastics: Dynamic Mechanical Properties: In Flexure (Three-Point Bending)*, West Conshohocken, PA.

[69] ASTM International, 2018, *E1641-18 Standard Test Method for Decomposition Kinetics by Thermogravimetry Using the Ozawa/Flynn/Wall Method*, West Conshohocken, PA.

[70] INTERNATIONAL STANDARD, 2020, *ISO/DIS 6452-2020 Rubber- or Plastics-Coated Fabrics — Determination of Fogging Characteristics of Trim Materials in the Interior of Automobiles*, Switzerland.

[71] Georgiopoulos, P., Kontou, E., and Christopoulos, A., 2015, "Short-Term Creep Behavior of a Biodegradable Polymer Reinforced with Wood-Fibers," Compos. Part B Eng., **80**, pp. 134–144.

[72] Kuzmanovic, M., Vanderbauwhede, S., Delva, L., Cardon, L., and Ragaert, K., 2016, "The Influence of Draw Ratio on Morphology and Thermal Properties of MFCs Based on PP and PET," (September).

[73] Franca, Z., 2019, "Automotive Upholstery2019," UNEWS. Inf. Mag., pp. 2–19.

[74] Mustapha, S., Ndamitso, M. M., Abdulkareem, A. S., Tijani, J. O., Mohammed, A. K., and Shuaib, D. T., 2019, "Potential of Using Kaolin as a Natural Adsorbent for the Removal of Pollutants from Tannery Wastewater," Heliyon, **5**(11), pp. e02923–e02923.

[75] Bar-Tal, A., Saha, U. K., Raviv, M., and Tuller, M., 2019, "Inorganic and Synthetic Organic Components of Soilless Culture and Potting Mixtures," *Soilless Culture: Theory and Practice Theory and Practice*, Elsevier, pp. 259–301.

[76] Zhang, N., Tao, P., Lu, Y., and Nie, S., "Effect of Lignin on the Thermal Stability of Cellulose Nanofibrils Produced from Bagasse Pulp," Cellulose, **26**.

[77] Wise, W. S., 2013, "MINERALS | Zeolites☆," *Reference Module in Earth Systems and Environmental Sciences*, Elsevier.

[78] Van Krevelen, D. W., and Te Nijenhuis, K., 2009, "Chapter 13 - Mechanical Properties of Solid Polymers," D.W. Van Krevelen, and K.B.T.-P. of P. (Fourth E. Te Nijenhuis, eds., Elsevier, Amsterdam, pp. 383–503.

[79] Yuan, Q., Wu, D., Gotama, J., and Bateman, S., 2008, "Wood Fiber Reinforced Polyethylene and Polypropylene Composites with High Modulus and Impact Strength," J. Thermoplast. Compos. Mater., **21**(3), pp. 195–208.

[80] Cruz, J., and Fangueiro, R., 2016, “Surface Modification of Natural Fibers: A Review,” Procedia Eng., **155**, pp. 285–288.

[81] Petinakis, E., Yu, L., Simon, G., Dai, X., Chen, Z., and Dean, K., 2014, “Interfacial Adhesion in Natural Fiber-Reinforced Polymer Composites,” *Lignocellulosic Polymer Composites: Processing, Characterization, and Properties*, pp. 17–39.

[82] Mohammed, L., Ansari, M. N. M., Pua, G., Jawaid, M., and Islam, M. S., 2015, “A Review on Natural Fiber Reinforced Polymer Composite and Its Applications,” Int. J. Polym. Sci., **2015**.

[83] Kozłowskiy, R., and Władyka-Przybylak, M., 2008, “Flammability and Fire Resistance of Composites Reinforced by Natural Fiber,” Polym. Adv. Technol., (November 2007), pp. 229–236.

APPENDIX A. CREO DRAWINGS OF FOGGING APPARATUS

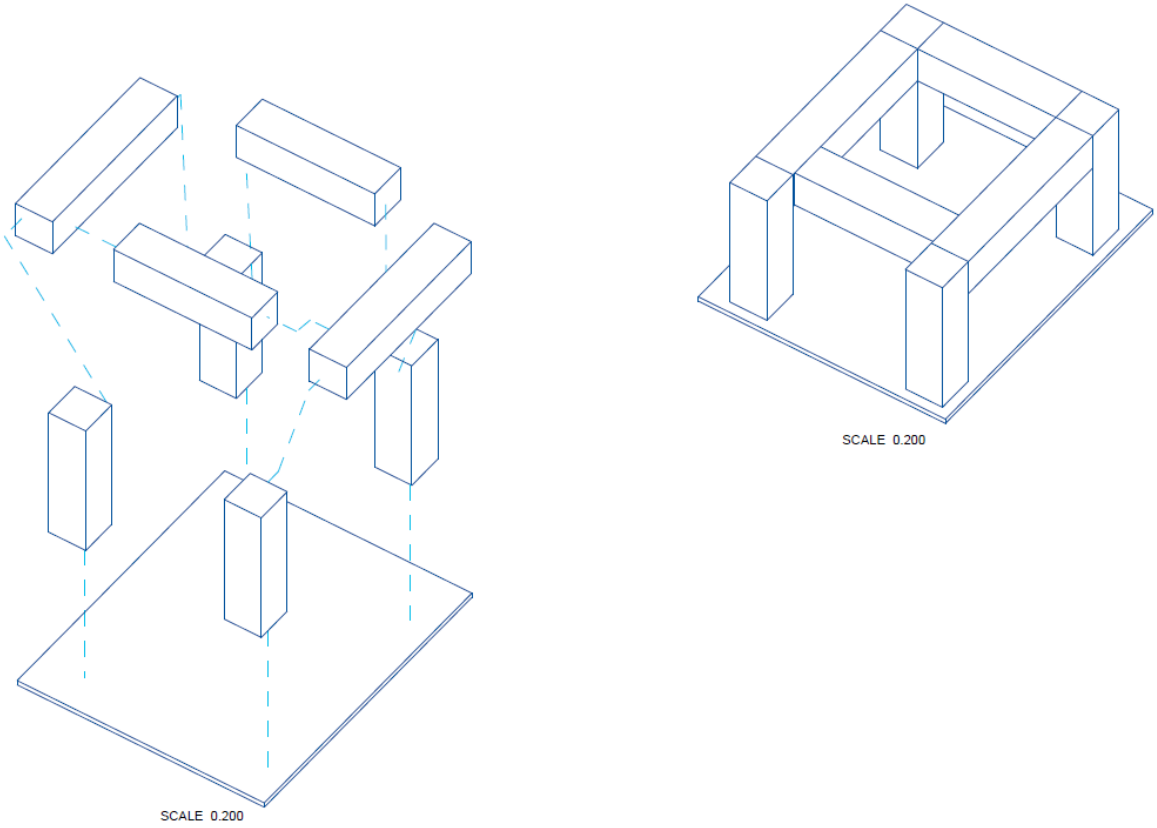

Figure A1. Frame of the fogging test

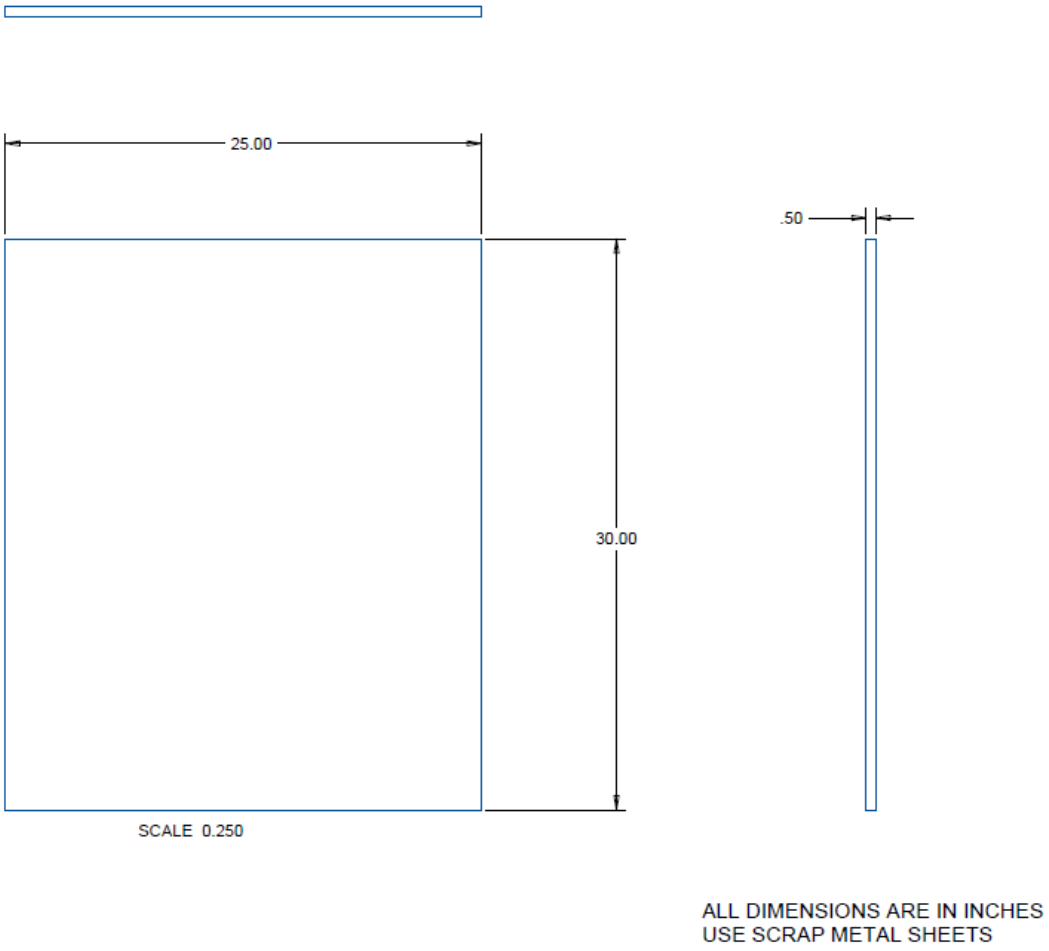

Figure A2. Base plate for the frame of the fogging test

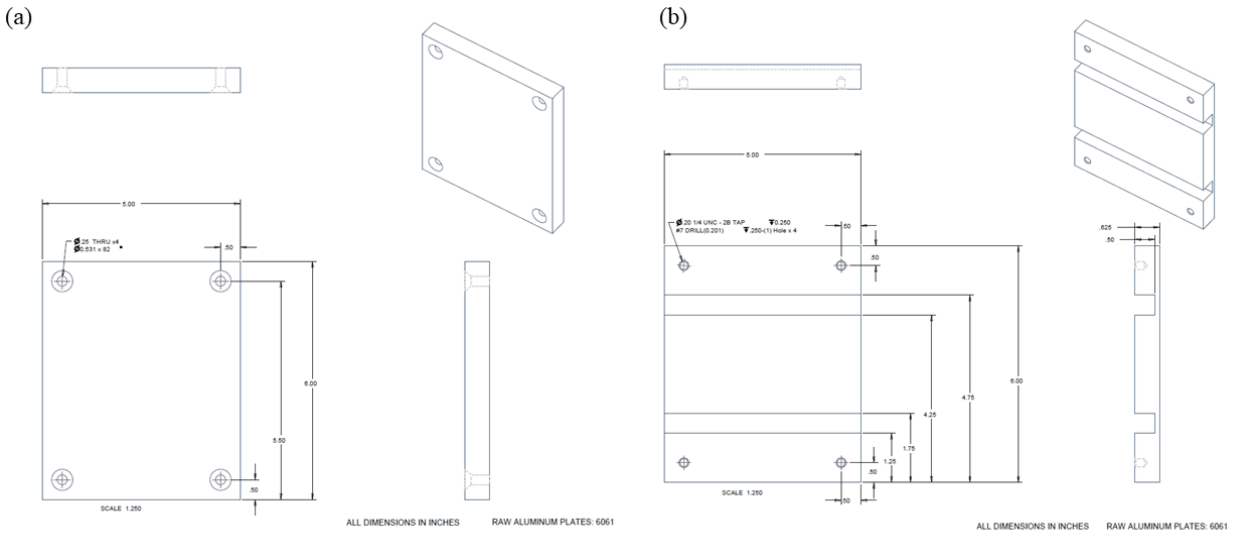

Figure A3. Creo drawings of the cooling plates (a) top part (b) bottom part

APPENDIX B. ANOVA STATISTICAL ANALYSIS OF DATA

Table B1. Statistical analysis, tensile strength for the Neat PP with and without porous fillers

SUMMARY

Groups	*Count*	*Sum*	*Average*	*Variance*
Neat PP	5	123.692	24.738	0.231
PSZ	5	136.847	27.369	0.405
PNZ	5	124.768	24.954	0.268
PVP	5	120.338	24.068	0.639
PWC	5	123.043	24.609	0.202

ANOVA: Single Factor

Source of Variation	*SS*	*df*	*MS*	*F*	*P-value*	*F crit*
Between Groups	32.992	4	8.248	23.631	2.44E-07	2.866
Within Groups	6.981	20	0.349			
Total	39.973	24				

Table B2. Statistical analysis, tensile strength for the 20%pine fiber-based composites with and without porous fillers

SUMMARY

Groups	*Count*	*Sum*	*Average*	*Variance*
20%PF	5	118.716	23.743	0.019
PPSZ	5	122.651	24.530	0.154
PPNZ	5	149.766	29.953	0.229
PPVP	5	145.496	29.099	1.494
PPWC	5	151.215	30.243	0.627

ANOVA: Single Factor

Source of Variation	*SS*	*df*	*MS*	*F*	*P-value*	*F crit*
Between Groups	195.160	4	48.790	96.713	8.66E-13	2.866
Within Groups	10.090	20	0.504			
Total	205.250	24				

Table B3. Statistical analysis, tensile strength for the 20%maple fiber-based composites with and without porous fillers

SUMMARY

Groups	*Count*	*Sum*	*Average*	*Variance*
20%MF	5	116.002	23.200	0.063
PMSZ	5	124.519	24.904	0.392
PMNZ	5	121.171	24.234	0.042
PMVP	5	116.793	23.359	0.925
PMWC	5	122.861	24.572	0.659

ANOVA: Single Factor

Source of Variation	*SS*	*df*	*MS*	*F*	*P-value*	*F crit*
Between Groups	11.177	4	2.794	6.710	0.001	2.866
Within Groups	8.328	20	0.416			
Total	19.505	24				

Table B4. Statistical analysis, tensile strength for the 20%flax fiber-based composites with and without porous fillers

SUMMARY

Groups	*Count*	*Sum*	*Average*	*Variance*
20%FF	3	82.807	27.602	0.086
PFSZ	5	142.915	28.583	0.707
PFNZ	5	147.645	29.529	0.207
PFVP	5	148.180	29.636	1.780
PFWC	5	147.132	29.426	0.488

ANOVA: Single Factor

Source of Variation	*SS*	*df*	*MS*	*F*	*P-value*	*F crit*
Between Groups	10.938	4	2.735	3.815	0.020	2.928
Within Groups	12.902	18	0.717			
Total	23.840	22				

Table B5. Statistical analysis, tensile modulus for the Neat PP with and without porous fillers

SUMMARY

Groups	*Count*	*Sum*	*Average*	*Variance*
Neat PP	5	8.611	1.722	0.015
PSZ	5	12.773	2.555	0.113
PNZ	5	11.223	2.245	0.050
PVP	5	11.146	2.229	0.014
PWC	5	11.671	2.334	0.021

ANOVA: Single Factor

Source of Variation	*SS*	*df*	*MS*	*F*	*P-value*	*F crit*
Between Groups	1.867	4	0.467	10.976	7.10E-05	2.866
Within Groups	0.851	20	0.043			
Total	2.718	24				

Table B6. Statistical analysis, tensile modulus for the 20%pine fiber-based composites with and without porous fillers

SUMMARY

Groups	Count	Sum	Average	Variance
20%PF	5	13.650	2.730	0.005
PPSZ	5	18.409	3.682	0.081
PPNZ	5	16.903	3.381	0.000
PPVP	5	16.818	3.364	0.004
PPWC	5	16.163	3.233	0.016

ANOVA: Single Factor

Source of Variation	SS	df	MS	F	P-value	F crit
Between Groups	2.416	4	0.604	28.493	5.23E-08	2.866
Within Groups	0.424	20	0.021			
Total	2.840	24				

Table B7. Statistical analysis, tensile modulus for the 20%maple fiber-based composites with and without porous fillers

SUMMARY

Groups	*Count*	*Sum*	*Average*	*Variance*
20%MF	5	14.272	2.854	0.013
PMSZ	5	19.160	3.832	0.040
PMNZ	5	18.959	3.792	0.021
PMVP	5	18.914	3.783	0.058
PMWC	5	19.821	3.964	0.028

ANOVA: Single Factor

Source of Variation	*SS*	*df*	*MS*	*F*	*P-value*	*F crit*
Between Groups	4.012	4	1.003	31.333	2.34E-08	2.866
Within Groups	0.640	20	0.032			
Total	4.652	24				

Table B8. Statistical analysis, tensile modulus for the 20%flax fiber-based composites with and without porous fillers

SUMMARY

Groups	*Count*	*Sum*	*Average*	*Variance*
20%FF	3	6.411	2.137	0.007
PFSZ	5	14.790	2.958	0.013
PFNZ	5	14.528	2.906	0.002
PFVP	5	15.516	3.103	0.021
PFWC	5	14.884	2.977	0.008

ANOVA: Single Factor

Source of Variation	*SS*	*df*	*MS*	*F*	*P-value*	*F crit*
Between Groups	1.985	4	0.496	45.859	3.34E-09	2.928
Within Groups	0.195	18	0.011			
Total	2.180	22				

Table B9. Statistical analysis, flexural strength for the Neat PP with and without porous fillers

SUMMARY

Groups	*Count*	*Sum*	*Average*	*Variance*
Neat PP	5	237.190	47.438	1.525
PSZ	3	193.590	64.530	9.680
PNZ	4	204.420	51.105	3.023
PVP	5	254.910	50.982	2.900
PWC	4	232.120	58.030	4.447

ANOVA: Single Factor

Source of Variation	*SS*	*df*	*MS*	*F*	*P-value*	*F crit*
Between Groups	685.374	4	171.344	46.099	1.38E-08	3.007
Within Groups	59.469	16	3.717			
Total	744.844	20				

Table B10. Statistical analysis, flexural strength for 20%pine fiber-based composites with and without porous fillers

SUMMARY

Groups	*Count*	*Sum*	*Average*	*Variance*
20%PF	5	267.760	53.552	2.241
PPSZ	5	259.630	51.926	2.064
PPNZ	5	262.260	52.452	1.059
PPVP	5	264.340	52.868	1.310
PPWC	5	265.750	53.150	0.759

ANOVA: Single Factor

Source of Variation	*SS*	*df*	*MS*	*F*	*P-value*	*F crit*
Between Groups	7.885	4	1.971	1.326	0.295	2.866
Within Groups	29.734	20	1.487			
Total	37.619	24				

Table B11. Statistical analysis, flexural strength for 20%maple fiber-based composites with and without porous fillers

SUMMARY

Groups	*Count*	*Sum*	*Average*	*Variance*
20%MF	5	259.680	51.936	7.209
PMSZ	5	261.080	52.216	1.063
PMNZ	5	262.390	52.478	0.555
PMVP	5	264.470	52.894	2.410
PMWC	5	262.540	52.508	0.513

ANOVA: Single Factor

Source of Variation	*SS*	*df*	*MS*	*F*	*P-value*	*F crit*
Between Groups	2.554	4	0.638	0.272	0.893	2.866
Within Groups	47.005	20	2.350			
Total	49.558	24				

Table B12. Statistical analysis, flexural strength for 20%flax fiber-based composites with and without porous fillers

SUMMARY

Groups	Count	Sum	Average	Variance
20%FF	5	256.250	51.250	0.836
PFSZ	5	259.000	51.800	0.285
PFNZ	5	261.680	52.336	0.683
PFVP	5	267.390	53.478	0.376
PFWC	5	269.610	53.922	1.947

ANOVA: Single Factor

Source of Variation	SS	df	MS	F	P-value	F crit
Between Groups	25.208	4.000	6.302	7.637	0.0007	2.866
Within Groups	16.504	20.000	0.825			
Total	41.712	24.000				

Table B13. Statistical analysis, flexural modulus for the Neat PP with and without porous fillers

SUMMARY

Groups	*Count*	*Sum*	*Average*	*Variance*
Neat PP	5	7.248	1.450	0.002
PSZ	3	11.428	3.809	0.035
PNZ	4	6.961	1.740	0.002
PVP	5	8.394	1.679	0.006
PWC	4	7.978	1.994	0.013

ANOVA: Single Factor

Source of Variation	*SS*	*df*	*MS*	*F*	*P-value*	*F crit*
Between Groups	12.123	4	3.031	329.048	3.85E-15	3.007
Within Groups	0.147	16	0.009			
Total	12.270	20				

Table B14. Statistical analysis, flexural modulus for the 20%pine fiber-based composites with and without porous fillers

SUMMARY

Groups	Count	Sum	Average	Variance
20%PF	5	12.909	2.582	0.016
PPSZ	5	11.541	2.308	0.020
PPNZ	5	11.236	2.247	0.016
PPVP	5	11.597	2.319	0.010
PPWC	5	11.697	2.339	0.020

ANOVA: Single Factor

Source of Variation	SS	df	MS	F	P-value	F crit
Between Groups	0.333	4	0.083	5.112	0.005	2.866
Within Groups	0.326	20	0.016			
Total	0.659	24				

Table B15. Statistical analysis, flexural modulus for the 20%maple fiber-based composites with and without porous fillers

SUMMARY

Groups	*Count*	*Sum*	*Average*	*Variance*
20%MF	5	11.119	2.224	0.005
PMSZ	5	11.042	2.208	0.011
PMNZ	5	10.821	2.164	0.005
PMVP	5	11.308	2.262	0.014
PMWC	5	10.755	2.151	0.004

ANOVA: Single Factor

Source of Variation	*SS*	*df*	*MS*	*F*	*P-value*	*F crit*
Between Groups	0.040	4	0.010	1.303	0.303	2.866
Within Groups	0.155	20	0.008			
Total	0.196	24				

Table B16. Statistical analysis, flexural modulus for the 20%flax fiber-based composites with and without porous fillers

SUMMARY

Groups	*Count*	*Sum*	*Average*	*Variance*
20%FF	5	10.011	2.002	0.001
PFSZ	5	9.794	1.959	0.003
PFNZ	5	9.863	1.973	0.005
PFVP	5	11.098	2.220	0.005
PFWC	5	11.231	2.246	0.007

ANOVA: Single Factor

Source of Variation	*SS*	*df*	*MS*	*F*	*P-value*	*F crit*
Between Groups	0.397	4	0.099	23.506	2.55E-07	2.866
Within Groups	0.084	20	0.004			
Total	0.481	24				

Table B17. Statistical analysis, impact strength for the Neat PP with and without porous fillers

SUMMARY

Groups	*Count*	*Sum*	*Average*	*Variance*
Neat PP	5	12.300	2.460	0.284
PSZ	4	44.149	11.037	1.791
PNZ	5	46.253	9.251	1.681
PVP	5	41.875	8.375	2.444
PWC	5	40.106	8.021	2.766

ANOVA: Single Factor

Source of Variation	*SS*	*df*	*MS*	*F*	*P-value*	*F crit*
Between Groups	196.651	4	49.163	27.412	1.17E-07	2.895
Within Groups	34.076	19	1.793			
Total	230.728	23				

Table B18. Statistical analysis, impact strength for the 20%pine fiber-based composites with and without porous fillers

SUMMARY

Groups	*Count*	*Sum*	*Average*	*Variance*
20%PF	5	11.171	2.234	0.029
PPSZ	5	21.704	4.341	0.252
PPNZ	5	21.145	4.229	0.120
PPVP	5	23.068	4.614	0.045
PPWC	5	22.162	4.432	0.322

ANOVA: Single Factor

Source of Variation	*SS*	*df*	*MS*	*F*	*P-value*	*F crit*
Between Groups	19.229	4	4.807	31.270	2.39E-08	2.866
Within Groups	3.075	20	0.154			
Total	22.304	24				

Table B19. Statistical analysis, impact strength for the 20%maple fiber-based composites with and without porous fillers

SUMMARY

Groups	*Count*	*Sum*	*Average*	*Variance*
20%MF	5	15.044	3.009	0.001
PMSZ	5	23.006	4.601	0.243
PMNZ	5	21.287	4.257	0.083
PMVP	5	26.985	5.397	0.274
PMWC	5	24.932	4.986	0.059

ANOVA: Single Factor

Source of Variation	*SS*	*df*	*MS*	*F*	*P-value*	*F crit*
Between Groups	16.607	4	4.152	31.469	2.26E-08	2.866
Within Groups	2.639	20	0.132			
Total	19.245	24				

Table B20. Statistical analysis, impact strength for the 20%flax fiber-based composites with and without porous fillers

SUMMARY

Groups	*Count*	*Sum*	*Average*	*Variance*
20%FF	5	16.733	3.347	0.022
PFSZ	5	26.768	5.354	0.075
PFNZ	5	25.786	5.157	0.413
PFVP	5	25.130	5.026	0.549
PFWC	5	26.626	5.325	0.065

ANOVA: Single Factor

Source of Variation	*SS*	*df*	*MS*	*F*	*P-value*	*F crit*
Between Groups	14.324	4	3.581	15.917	5.24E-06	2.866
Within Groups	4.500	20	0.225			
Total	18.824	24				

Table B21. Statistical analysis, F test for the Neat PP with and without porous fillers

SUMMARY

Groups	*Count*	*Sum*	*Average*	*Variance*
Neat PP	2	146.770	73.385	2.100
PSZ	2	177.426	88.713	5.258
PNZ	2	176.690	88.345	0.178
PVP	2	165.260	82.630	0.092
PWC	2	178.463	89.231	4.132

ANOVA: Single Factor

Source of Variation	*SS*	*df*	*MS*	*F*	*P-value*	*F crit*
Between Groups	363.907	4	90.977	38.682	5.93E-04	5.192
Within Groups	11.759	5	2.352			
Total	375.666	9				

Table B22. Statistical analysis, F test for the 20%pine fiber-based composites with and without porous fillers

SUMMARY

Groups	*Count*	*Sum*	*Average*	*Variance*
20%Pine	2	160.214	80.107	4.940
PPSZ	2	178.546	89.273	3.058
PPNZ	2	179.100	89.550	0.870
PPVP	2	183.380	91.690	1.437
PPWC	2	169.509	84.754	1.416

ANOVA: Single Factor

Source of Variation	*SS*	*df*	*MS*	*F*	*P-value*	*F crit*
Between Groups	172.384	4	43.096	18.384	0.003	5.192
Within Groups	11.721	5	2.344			
Total	184.105	9				

Table B23. Statistical analysis, F test for the 20%maple fiber-based composites with and without porous fillers

SUMMARY

Groups	*Count*	*Sum*	*Average*	*Variance*
20%Maple	2	170.212	85.106	10.716
PMSZ	2	172.756	86.378	6.524
PMNZ	2	178.066	89.033	0.726
PMVP	2	166.422	83.211	2.064
PMWC	2	172.337	86.169	3.159

ANOVA: Single Factor

Source of Variation	*SS*	*df*	*MS*	*F*	*P-value*	*F crit*
Between Groups	35.886	4	8.972	1.934	0.243	5.192
Within Groups	23.189	5	4.638			
Total	59.075	9				

Table B24. Statistical analysis, F test for the 20%flax fiber-based composites with and without porous fillers

SUMMARY

Groups	*Count*	*Sum*	*Average*	*Variance*
20%Flax	2	172.704	86.352	16.258
PFSZ	2	176.870	88.435	0.013
PFNZ	2	175.133	87.566	8.783
PFVP	2	178.559	89.280	0.002
PFWC	2	178.186	89.093	0.015

ANOVA: Single Factor

Source of Variation	*SS*	*df*	*MS*	*F*	*P-value*	*F crit*
Between Groups	11.640	4	2.910	0.580	0.691	5.192
Within Groups	25.072	5	5.014			
Total	36.712	9				

Table B25. Statistical analysis, G test for the Neat PP with and without porous fillers

SUMMARY

Groups	*Count*	*Sum*	*Average*	*Variance*
ID	2	3.000	1.500	0.500
Neat PP	2	2.100	1.050	0.005
PSZ	2	1.300	0.650	0.005
PNZ	2	1.100	0.550	0.005
PVP	2	1.700	0.850	0.005
PWC	2	1.600	0.800	0.020

ANOVA: Single Factor

Source of Variation	*SS*	*df*	*MS*	*F*	*P-value*	*F crit*
Between Groups	1.160	5	0.232	2.578	0.140	4.387
Within Groups	0.540	6	0.090			
Total	1.700	11				

Table B26. Statistical analysis, G test for the 20%pine fiber-based composites with and without porous fillers

SUMMARY

Groups	*Count*	*Sum*	*Average*	*Variance*
20%Pine	2	2.900	1.450	0.005
PPSZ	2	1.800	0.900	0.020
PPNZ	2	2.000	1.000	0.020
PPVP	2	2.100	1.050	0.005
PPWC	2	1.500	0.750	0.005

ANOVA: Single Factor

Source of Variation	*SS*	*df*	*MS*	*F*	*P-value*	*F crit*
Between Groups	0.546	4	0.137	12.409	0.008	5.192
Within Groups	0.055	5	0.011			
Total	0.601	9				

Table B27. Statistical analysis, G test for the 20%maple fiber-based composites with and without porous fillers

SUMMARY

Groups	*Count*	*Sum*	*Average*	*Variance*
20%Maple	2	2.300	1.150	0.005
PMSZ	2	2.000	1.000	0.020
PMNZ	2	1.900	0.950	0.005
PMVP	2	2.200	1.100	0.020
PMWC	2	1.700	0.850	0.005

ANOVA: Single Factor

Source of Variation	*SS*	*df*	*MS*	*F*	*P-value*	*F crit*
Between Groups	0.114	4	0.029	2.591	0.162	5.192
Within Groups	0.055	5	0.011			
Total	0.169	9				

Table B28. Statistical analysis, G test for the 20%flax fiber-based composites with and without porous fillers

SUMMARY

Groups	*Count*	*Sum*	*Average*	*Variance*
20%Flax	2	3.700	1.850	0.045
PFSZ	2	2.300	1.150	0.045
PFNZ	2	2.100	1.050	0.045
PFVP	2	2.600	1.300	0.020
PFWC	2	2.200	1.100	0.020

ANOVA: Single Factor

Source of Variation	*SS*	*df*	*MS*	*F*	*P-value*	*F crit*
Between Groups	0.854	4	0.214	6.100	0.037	5.192
Within Groups	0.175	5	0.035			
Total	1.029	9				